(19) Europäisches Patentamt
European Patent Office
Office européen des brevets

(11) **EP 4 324 982 A1**

(12) **EUROPEAN PATENT APPLICATION**
published in accordance with Art. 153(4) EPC

(43) Date of publication:
21.02.2024 Bulletin 2024/08

(21) Application number: **22758653.4**

(22) Date of filing: **23.02.2022**

(51) International Patent Classification (IPC):
E01B 2/00 *(2006.01)* ***E01B 5/14*** *(2006.01)*

(86) International application number:
PCT/BY2022/000003

(87) International publication number:
WO 2022/178612 (01.09.2022 Gazette 2022/35)

(84) Designated Contracting States:
AL AT BE BG CH CY CZ DE DK EE ES FI FR GB GR HR HU IE IS IT LI LT LU LV MC MK MT NL NO PL PT RO RS SE SI SK SM TR
Designated Extension States:
BA ME
Designated Validation States:
KH MA MD TN

(30) Priority: **23.02.2021 EA 202100109**

(71) Applicant: **Velichko, Gennady Viktorovich**
Minsk, 220014 (BY)

(72) Inventor: **Velichko, Gennady Viktorovich**
Minsk, 220014 (BY)

(74) Representative: **Vossius & Partner**
Patentanwälte Rechtsanwälte mbB
Siebertstrasse 3
81675 München (DE)

(54) TRANSITION SECTION OF A RAILWAY TRACK CURVE

(57) The present invention relates to the configuration and use of a transition section of a curve in a railway track, the novel relationships of the harmonizable shape of which provide for high quality cornering movement of a railway vehicle through said section at a set speed *V*, where, with respect to a length *l*, the curvature of the axis of the track *k*(*l*) in said section and the transverse inclination *i*(*l*) of the track are variable.

The shape of the track axis in the transition section is determined by the position N of equidistant points having the coordinates *x*[*n*] and *y*[*n*], which are determined using formulas (1) and (2), the variables of which are determined in turn using formulas (3)-(5). The transverse inclination i[n] of the track at these points is determined using formula (6), the variables of which are determined in turn using formulas (7)-(9). Alongside the traditional controlled parameter *L* (length of the transition section), the present invention envisages the additional possibility of variation of the values of the controlled parameters *Z* and *U*, which have an effect on the overall geometric properties of the non-identity functions of an angle, the curvature and the transverse inclination of the track in the transition section.

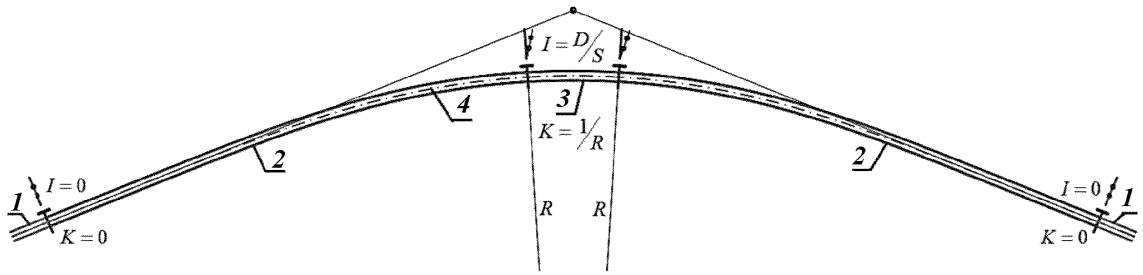

FIG. 1

EP 4 324 982 A1

Description

[0001] The present invention relates to the configuration and use of a transition section (TS) of a curve in a railway track, with the novel relationships of the harmonizable shape thereof accounting for a high quality of the cornering movement of the railway vehicle through said section, travelling at the set speed *V*, with the length *l,* curvature *i*(*l*) of the track axis *k*(*l*), and transverse inclination being variables.

[0002] The rail (track) route plan consists of a succession of alternating linear sections and curves inscribed within their roll angles. Every curve consists of a circular and two transition sections of the length *L.* The circular section axis is defined with a radial arc $K = 1/R$, with the outer rail being superelevated above the inner one by the constant value *D*. This enables partial reduction of the transversal acceleration, to which the circular portion of the curve is exposed at the estimated speed *V*. This reduction can be achieved by providing a transverse inclination that is directed toward the center of its curvature $I = D/S$. The slope remains constant within the circular section of the curve, for all along the curve section it is only dependent on the superelevation *D* and rail gauge *S.* The parameters *V, R, D* and *S* remaining constant within the circular section of the rail curve make sure that the highest possible theoretical value of undampened sway acceleration (USA) a_{max} remains constant. The concurrence of *V, R, D* and *S* makes sure that there's a balance between the value generated by the said parameters, and the permissible value $a_{\partial on}$, which is subject to the condition $a_{max} \leq a_{\partial on}$. USA a_{max} is calculated as the product of vectorial addition of gravitational *G* and centrifugal C accelerations $a_{max} = C - G \cdot \tan(\alpha)$, arising in the horizontal plane, where α is the transverse inclination of the track, calculated as $\alpha = \arcsin(I)$.

[0003] Unlike the track curve, the transition section is more complex in shape. It depends on the formula for the curvature $k(\chi)$ and transverse inclination $i(\chi)$ function, varying within the $0 \leq k(\chi) \leq$ and $0 \leq i(\chi) \leq I$ range depending on the relative share of the current track length $\chi = l / L$ that is continuously varying within the $0 \leq \chi \leq 1$ range. The functions of the majority of TS shapes of the prior art are disclosed in publications [1-4]. For each and every one of them, the relationship of its curvature $k(\chi)$ and transverse inclination $i(\chi)$ is uniformly defined in accordance with the principle $k(\chi) = K \cdot f(\chi)$ and $i(\chi) = I \cdot f(\chi)$ in line with the criterion $0 \leq f(\chi) \leq 1$. The said principle predetermines the identity of the characteristics of the curvature and transverse inclination graphs for the majority of the existing TS shapes of the prior art. Please note that the main difference lies in the geometric smoothness order G^n of strictly monotonous unit functions $f(\chi)$. It defines the maximum order of differences between zero and the n^{th} derivative, which takes zero at points $\chi = 0$, and $\chi = 1$. The widely used TS shape with the G^0 th order of smoothness has a function that is $f(\chi) = \chi$. This is the reason why the graphs of the relationships its curvatures $k(\chi)$ and transverse inclination $i(\chi)$ take the form of straight lines $k(\chi) = \chi \cdot K$ and $i(\chi) = \chi \cdot I$. The relationships of relative Cartesian coordinates $x(\chi)$ and $y(\chi)$ of the horizontal projection of the track axis of the said TS shape correspond to only one flat curve, defined in the prior art as *clothoid* or *spiral.*

[0004] All other TS shapes of the $G^{n_{th}}$ smoothness order with $n > 0$ have smooth contours of the relationships of the curvature thereof $k(\chi)$ and transverse inclination $i(\chi)$ that are similar to the first half of the sine curve chart. This is what the common name for their shapes i.e. *half-sine* is predicated upon. Half-sine TS shapes that have the same order of smoothness, have various relationships of function $f(\chi)$. They differ by their smoothness, which is assessed by the maximum of their first derivative $d\, f(\chi)/d\, \chi$ calculated at the point $\chi = 0.5$.

[0005] The use of *half-sine* TS shapes rendered the issue of the so-called *lateral jerk* occurring at the beginning and at the end of a clothoid TS less acute. However, their operation revealed motion quality issues, caused by low-frequency oscillations of railway vehicles. This becomes evident from the research conducted at the end of the last century in Japan on TS [5] of straights and curves of high-speed railway lines. As traveling speeds grow higher, and high-speed railway lines (HSRL) get more advanced, the problem of pivotal movement of the railway vehicles caused by a changes in the curvature of the TS axis and transverse inclination of the track, grew more severe. This is indicated by the ogling trend to make the relationships of the TS *half-spine* shapes more complex in order to reduce the maxima of the first derivatives of their functions $d\, f(\chi)/d\, \chi$ in their central part [3]. Besides one also uses the so called "elevated routing" [2,3], whereby the relationship of curvature $k(\chi) = K \cdot f(\chi)$ defines the trajectory of motion of the railway vehicle reference point that is superelevated above the top of rail (TOR) by the height H, rather than the TS track axis.

[0006] Normally, the variety of such measures is designed to address the main issue encountered in the operation of the "Track + Railway Vehicle" (TRV), which manifests itself on the railway track curves as an adverse force interaction between its elements and reduced comfort of the passenger ride. This causes an increase in the rates at which the geometry of the TS track and adjacent sections gets compromised, as well as premature wear of the rails and railway vehicle wheels. The extent of destructive effect of such processes is to a larger degree dependent on geometrical properties of the TS shapes. Kinematic tests of TRV on TS with both conventional and cutting-edge shapes [6] reveal that each is flawed in some way or the other and fails to provide the required quality of curvilinear railway vehicle motion. However, even the EU standard fails to list theoretically substantiated priorities for selection and application of one of five recommended TS shapes that would provide the highest TRV operation quality.

[0007] The existing issues of substantiating and hands-on application the majority of TS shapes of the prior art are accounted for by insufficiently adequate and oversimplified TRV system models, as well as techniques employed to assess the quality of their operation. These are normally based on the kinematics of an abstract point located on the

level of TOR. By contrast, the provisions hereof are based on the kinematic performance of points located at the railway vehicle levels that are functionally significant. Given the mode of transportation and priority quality aspects, the estimated levels where these can be located, factor in the location of the railway vehicle's center of mass (COM) and/or the position of its passenger's vestibular apparatus.

[0008] This approach chimes in with the goal of assuring the curvelinear railway vehicle motion quality, which is conventionally assumed to mean an acceptable level of passenger comfort and smooth changes in the interaction between the railway vehicle wheels and rail tracks. However, to make sure that such level is achieved through the use of any TS shape of the prior art, one was only left with the option of varying the length values *L* only. Moreover, the simplified TRV system rendered it impossible to objectively assess the impact of this factor on its operation in such sections.

[0009] The tests conducted on the Japanese railways revealed that the discomfort and adverse effect on the passenger health is caused by low-frequency oscillations of side acceleration with frequencies under 1 Hz [5]. According to the calculation data obtained using the multifactor deterministic kinematic model (MDKM) described in the paper [6] , the said nature of sway accelerations that are found to affect the railway vehicle at the predicted level $H > 0$, is in one way or the other inherent in all TS *half-sine* shapes of the prior art. This reveals itself in the form of considerable oscillation amplitudes of values of their USA formulas $a(l)$, and speeds at which these change $\psi = da/dt$, TS travel length / and time t variables. The same oscillations result in an uneven distribution of reaction forces, which drives up the dynamic component of the load to which they are exposed.

[0010] The values and relationships of such parameters depend on a complex interaction of various geometric and physical factors to which they are exposed, with the most crucial effect thereof manifesting itself and being assessed at the predicted level *H* of the railway vehicle. This explains the integrative nature of the said parameters, which is substantially different from the local kinematic parameters of the abstract point that are conventionally calculated and assessed in the prior art at TOR = 0. The complexity of interactions between the TRV system components is factored in its multifactor deterministic kinematic model (MDKM) described in the paper [6]. The integrative parameters exhibitive of the quality of its operation, calculated in MDKM, are dependent on the values of the following parameters:

- railway vehicle speed *V*;
- circular curve radius *R*;
- estimated rail cant *D*;
- distance between the rail axes *S*;
- superelevation of the reference point H above TOR;
- TS length *L*;
- relationship $\beta(l)$ of the angle tangent relative to the track axis and its curvature $k(l)$;
- relationship of offset of the track transverse inclination $i(l)$;
- relationship of curvature of the projected trajectory of motion of the reference point $k_H(l)$ onto a horizontal plane;
- value taken by the Boolean variable depending on whether the outer rail is symmetrically (*true*) or asymmetrically (*false*) elevated above the inner one.
- relationship of curvature of the track axis projection onto a vertical plane $k_V(l)$;
- relationship of curvature of the outer (left) rail longitudinal axis projection onto a vertical plane $k_L(l)$;
- relationship of curvature of the inner (right) rail longitudinal axis projection onto a vertical plane $k_R(l)$;

[0011] The analysis of data obtained through the use of MDKM [6], revealed variations within the acceptable range only for TS lengths *L* of the prior art which prevents alignment of the above-listed characteristics of their *half-sine* shapes in a way that allows to eliminate or reduce the amplitude of oscillations of the USA functions inherent therein $a(l)$, or speeds at which they change $\psi = da/dt$. This makes it impossible to ensure that the difference between the reaction forces of the outer and inner rails $\Delta F = F_L - F_R$ grows uniformly and smoothly.

[0012] The nature of such flows that are hard to eliminate and pertain to the TS *half-sine* shapes exemplifies assessment of the integral quality parameters of one of the best TS shapes [3], described in *Order (3, 7).* Out of the alternatives proposed in [3] it has the highest G^{4th} order of smoothness. The chart of the 1st derivative function of the offset of the track cross-slope and curvature of its axis shows a distinctive "plateau" (see Fig. 9). This is a clear indication that the author of the solution sought to eliminate the amplitude of USA oscillations $a(l)$, and lower the maximum constant speed at which it changes ψ_{max} for a larger portion of TS. However, as the kinematic analysis of the use of TRV on TS of the said shape suggests, accomplishment of the said goal will bring about a substantial dispersion of other parameters or other integrative motion quality parameters at the beginning and at the end thereof (see Fig. 10 - 13).

[0013] Therefore, the primary items to be used in the assessment of TS obtained in this way or the other, are the diagrams of distribution of USA $a(l)$ and speeds at which it changes $\psi(l)=da/dt$, applying at the reference level *H.* The quasilinearity of the USA $a(l)$ distribution diagram is exhibitive of a high quality of the TS configuration that is assured under the condition that the curve of velocity at which it changes is smooth $\psi(l)=da/dt$ as it approaches its central, plateau-

like section. It follows that the comfort of moving passengers, and positive force interaction of the TRV system elements must be ensured through smooth change of curves *a(l), and* $\psi(l)$ existing at the railway vehicle levels that are critical for every parameter impacting the quality of its motion. The priority of passenger comfort necessitates linearization of the curve $\psi(l)$ for a longer portion of the central TS section, ensuring a minimum deviation of the constant minimum values

$$\psi_{MIN} \approx \frac{v}{L}\left(\frac{v^2}{R} - g\frac{D}{S}\right)$$

ψ_{max} of its curve from the absolute minimum that is practically unattainable .

[0014] Based on the totality of technical attributes, the claimed TS shape of the rail track curve is the closest to the one described in "Railroad curve transition spiral design method based on control of vehicle banking motion", by *Order (3,7)* [3]. The method of designing a transition rail track curve, disclosed therein, implies selection of one out of 18 mathematical expressions defining acceleration (i.e. second derivative) of the transverse inclination angle (banking motion) depending on the variable distance, varying from naught to the set length of the transition curve. The selected mathematical expression determines the geometrical properties of the shape of the TS track axis with the *L* length and its transverse inclination. Due to lack of methodology and functionally substantiated criteria for selecting the required mathematical expression, or assignment of the TS length *L*, or additional parameters that are oftentimes required, the transition section shape provided by the aforesaid invention fails to eliminate flaws inherent in the prior art.

[0015] To identify such flaws or look for ways to eliminate the same through adoption of a new TS shape that has a geometry to fit the purpose, one relied on a more advanced kinematic model of the curvilinear railway vehicle motion with variable curvature of the track axis and its transverse inclination [6].

[0016] Analyses of TS shapes of the prior art [6] made it possible to formulate the objective of the present invention, which comes down to establishment of patterns of the track shape and length *L* of the railway curve TS, which if observed during the design and construction phases, will allow to achieve the highest operating quality of the TRV system at the given values of the following parameters: motion speed *V*, curve radius *R,* cant *D,* superelevation of the reference point *H* above TOR, and distance between the rail axes *S.* Therefore, the technical outcome of the claimed invention must be the achievement of the highest operating quality of the TRV system on the railway curve provided that its design parameters are observed.

[0017] The task at hand can be resolved, and the foregoing technical performance can be achieved through use of the claimed transition section of the rail track curve, which along the length *L* integrates the adjoining straight section and the circular section of the curve with the constant radius *R,* encompassing the base and track-forming rail-tie grid, resting thereon in full accordance with the coordinates of the projection of transition section points onto a horizontal plane with a variable transverse inclination *i* varying along the length *L* that is normal to the axis line that is tangent to the top of rail, with the track axis shape of the transition section being dependent on the location *N* of equidistant points with the coordinates *x*[*n*] and *y*[*n*], and the transverse inclination *i*[*n*] of the track at such points varying along the transition section axis in the range of $0 \le i[n] \le D/S$, where *D* is the estimated superelevation of the outer rail above the inner one within the rail track curve, and S is the distance between the vertical axes of the rail track cross section, as $\Delta_l = L/(N-1)$ the distance *l*[*n*] between each n^{th} point and *l*[0] = 0.0 m increases proportionately by a constant, at the beginning of the transition section axis, and up to *l*[*N* -1] = *L* at the section's end. The task at hand is resolved, and the foregoing technical performance can be achieved by establishing the relative rectangular coordinates of the track axis projection points *x*[*n*] and *y*[*n*] using the formulas:

$$x[0] = 0.0; \qquad x[n] = x[n-1] + \Delta_l \cdot \cos\left(\beta_b(\delta) + \Delta_\beta(\delta)\right) \qquad (1),$$

$$y[0] = 0.0; \qquad y[n] = y[n-1] + \Delta_l \cdot \sin\left(\beta_b(\delta) + \Delta_\beta(\delta)\right) \qquad (2),$$

where:

n is the reference number of the transition section axis point varying within the $1 \le n \le (N-1)$ range,
x[*n*] is the coordinate that characterizes the distance between the start of transition section and location of the n^{th} axis point projected onto a line that is tangent thereto at point *x*[0] and *y*[0],
y[*n*] is a coordinate that characterizes the shift towards the curvature center of the n^{th} axis point normally from the line that is tangent thereto at point *x*[0] and *y*[0],
Δ_l is the transition section length/ track axis complement constant, measured in an arc from its start to each n^{th} point,
δ is the relative percentage of the current length $l + \Delta_l/2$ of the transition section track axis, measured from its start

to the middle of the axis section, confined between its adjacent points *n*-1 and *n*, calculated by the formula:

$$\delta = \frac{2n-1}{2(N-1)} \quad (3),$$

β_b (δ) is the value of the base angle function of the tangent to the transition section calculated in accordance with the relative percentage of the δ current length *l* + Δ_l/2 up to the point of contact, using the formula:

$$\beta_b(\delta) = \frac{L}{R}\delta^6\left(\frac{315}{6} - \delta\left(\frac{2043}{7} - \delta\left(\frac{6720}{8} - \delta\left(\frac{14085}{9} - \delta\left(\frac{19795}{10} - \delta\left(\frac{18579}{11} - \delta\left(\frac{11178}{12} - \delta\left(\frac{3900}{13} - \frac{600}{14}\delta\right)\right)\right)\right)\right)\right)\right)\right) \quad (4),$$

' is the value of the complement base angle function of the tangent to the transition section calculated in accordance with the relative percentage of the δ current length *l* + Δ_l/2 up to the point of contact, using the formula:

$$\Delta_\beta(\delta) = U\frac{L}{R}\delta^6\left(\frac{7}{6} - \delta\left(\frac{74}{7} - \delta\left(\frac{340}{8} - \delta\left(\frac{885}{9} - \delta\left(\frac{1425}{10} - \delta\left(\frac{1452}{11} - \delta\left(\frac{914}{12} - \delta\left(\frac{325}{13} - \frac{50}{14}\delta\right)\right)\right)\right)\right)\right)\right)\right) \quad (5),$$

where
U is the parameter establishing the base angle complement of the tangent to the transition section axis at its every point with a relative percentage δ of its current length *l* + Δ_l/2

[0018] The transverse inclination *i*[*n*] of the transition section track at the n^{th} point of its axis varying within the interval $0 \le n \le (N-1)$ is determined using the formula

$$i[n] = i_b(\chi) + \Delta_i(\chi) \quad (6),$$

where

χ is the relative percentage of the track length/axis to point *n*, calculated as:

$$\chi = \frac{n}{N-1} \quad (7),$$

$i_b(\chi)$ is the value of the function of the base track transverse inclination of the transition section calculated in accordance with the relative percentage χ, using the formula:

$$i_b(\chi) = \frac{D}{S}\chi^4\left(37 - \chi\left(102 - \chi\left(140 - \chi\left(172 - \chi\left(198 - \chi\left(154 - \chi\left(66 - 12\chi\right)\right)\right)\right)\right)\right)\right) \quad (8),$$

$\Delta_i(\chi)$ is the value of the function of the complement to the track transverse inclination at *n*, calculated in accordance with the relative percentage χ, using the formula:

$$\Delta_i(\chi) = -Z\frac{D}{S}\chi^4\left(1 - \chi\left(9 - \chi\left(35 - \chi\left(76 - \chi\left(99 - \chi\left(77 - \chi\left(33 - 6\chi\right)\right)\right)\right)\right)\right)\right) \quad (9),$$

where:
Z is the parameter establishing the complement to the primary transverse inclination of the track at its every point

with the relative percentage χ.

[0019] Practical experience teaches that combinations of predetermined *V, R, D, S,* and *H* parameters of the TRV system can be galore. This is a substantial obstacle on the way to addressing the task of maintaining a stable high operating quality of TRV system, given the substantial differences in the values characteristic of various combinations. Research [7] shows that the highest coordination between the TRV system elements is achieved through fine-tuning of the final geometric properties of the TS shape $\beta\left(\frac{l}{L}\right)$, and $i\left(\frac{l}{L}\right)$ by relying on complements $\Delta_\beta\left(\frac{l}{L}\right)$ and $\Delta_i\left(\frac{l}{L}\right)$. . The values of such compliments depend on the difference between the current combination of the design parameters *V, R, D, S,* and *H,* and the option that was factored in whilst substantiating the basic properties of the TS shape $\beta_b\left(\frac{l}{L}\right)$ and $i_b\left(\frac{l}{L}\right)$.

[0020] Therefore, in addition to the controlled parameter *L*, the present invention additionally makes it possible to vary the values of the controlled parameters *Z* and *U*, which impact the ultimate geometric properties of the non-identical functions of the angle, curvature, and transverse inclination of the TS track. At each point of its axis that is removed from its start at the distance *l*, this impact is implemented through the dependence of its coordinates *x*(*l*) and *y*(*l*) on the function of the angle tangent to it $\beta\left(\frac{l}{L}\right)$, consisting of the primary value $\beta_b\left(\frac{l}{L}\right)$ calculated by formula (4), and complement thereto $\Delta_\beta\left(\frac{l}{L}\right)$, designated as *U* and dependent thereon, which is calculated by formula (5), and also due to the dependence of the current superelevation *d*(*l*) of the outer rail above the inner one, corresponding to this point, on the track cross sloe function $i\left(\frac{l}{L}\right)$, comprised of the primary value $i_b\left(\frac{l}{L}\right)$ calculated by formula (8), and the complement Z thereto $\Delta_i\left(\frac{l}{L}\right)$, which depends on it and is calculated using the formula (9).

[0021] The minimum and maximum degrees of the members of the polynomial functions (4), (5), (8), and (9), and coefficients thereof, as well as ranges of values of the controlled parameters Z, and *U*, are substantiated based on the strict monotonicity of the G^4 -smooth track axis curvature functions, described by the first derivative of the tangent angle function in terms of the TS length $k\left(\frac{l}{L}\right)=d\left(\beta_b\left(\frac{l}{L}\right)+\Delta_\beta\left(\frac{l}{L}\right)\right)\Big/dl$, and the G^3 smooth track transverse inclination function $i\left(\frac{l}{L}\right)$ that is non-identical to it. With χ = *l*/L the TS axis curvature function *k*(χ) at each current length/TS coordinate is defined as

$$k(\chi)=k_b(\chi)+\Delta_k(\chi) \qquad (10),$$

where

$$k_b(\chi)=\frac{L}{R}\chi^5\left(315-\chi\left(2043-\chi\left(6720-\chi\left(14085-\chi\left(19795-\chi\left(18579-\chi\left(11178-\chi\left(3900-600\chi\right)\right)\right)\right)\right)\right)\right)\right) \qquad (11),$$

$$\Delta_k(\chi) = U\frac{L}{R}\chi^5\left(7-\chi\left(74-\chi\left(340-\chi\left(885-\chi\left(1425-\chi\left(1452-\chi\left(914-\chi\left(325-50\chi\right)\right)\right)\right)\right)\right)\right)\right) \quad (12),$$

U is a parameter establishing the highest complement to the primary transition section track curvature axis.

[0022] This mathematical description of the functions (4), (5), (8), (9), (11), (12) substantially expands the possibility for coordination of all TRV system properties, thus providing a stably high level of operating quality for any recommended combinations of its predetermined *V, R, D, H, S,* and controlled *L, Z, U* parameters. As used herein, the process for assuring such coordination, is referred to as harmonization, and the resulting TS shape is referred to as harmonized, and the controlled *L, Z,* and *U* parameters corresponding thereto are considered optimal.

[0023] The quasilinear G^1 smooth USA curve *a*(*l*), associated with the desired level of TRV operating quality on the harmonized shape TS needs to correspond to the G^0 smooth speed change diagram $\psi(l) = da/dt$. Satisfaction of the said requirement eliminates the so-called *lateral jerk* occurring at the beginning and at the end of TS. This said, the maximum speed maintained throughout a substantial portion of the central TS section needs to be constant. Ideally, if all of the foregoing requirements are satisfied, the contours of the diagram $\psi(l)$ will resemble the outline of an equicrural trapezoid with rounded off angles and a quite extensive "plateau" in its central part. Such an outline is the most conducive to nearing the "plateau" line with constant values ψ_{max} to the absolute but almost unattainable minimum ψ_{MIN}. This fits in within the common belief on maintaining the highest quality of motion.

[0024] The *half-sine* TS shapes of the prior art have intrinsical low-frequency oscillations of the integrative kinematic parameters at the design railway vehicle level *H*. This is corroborated by the data of tests using MDKM [6]. The magnitude and frequency of such oscillations depend on the incongruent interaction of the identical properties of non-linear relationships of the track cross-slope offset and the curvature of the track axis. The TS configuration that is of the shape claimed in this invention makes it possible to substantially reduce the amplitudes of such oscillations to practically negligible levels. However, the "stability", and degree of approximation of ψ_{max} to ψ_{MIN} within the diagram "plateau" $\psi(l)$ need to be assessed on the basis of dispersion *W* of the speeds at which values $d\psi/dt$ change from the zero speed ψ_{max}, which represents stability. This suggests that the synergies achieved for various combinations of the predetermined *V, R, D, H, S* values, and controlled *L, Z, U* TRV system parameters, is reversely proportional to the dispersion *W*. Accordingly, the target of searching for the optimal *L, Z,* and *U* parameters is formalized as:

$$\frac{1}{M}\sum_{\delta=\delta_b}^{\delta=\delta_e}\left(\frac{d\psi(\delta)}{dt}\right)^2 \Rightarrow \min \quad (13),$$

where

δ_b is the relative percentage of the plateau start as shown on the function diagram $\psi(l)$;
δ_e is the relative percentage of the plateau end as shown on the function diagram $\psi(l)$;
M is the number of points with relative length percentages δ, evenly distributed within the δ_b to δ_e interval, wherein one conducts numeric assessment of the oscillation amplitude of the function values $d\psi/dt$;

[0025] Due to external factors, no solution to the task can neutralize the adverse impact produced by the relationship of the vertical curvature of the TS axis and/or asymmetric (see Fig. 16, 17) superelevation offset *D*. Therefore, the target function (13) needs to be minimized regardless of such factors, i.e. at the hypothetically zero vertical curvature of the TS axis, and symmetric (see Fig. 14, 15) superelevation offset *D*. The analytical MDKM dependencies [6] reveal that for the symmetric superelevation offset *D* the vertical curvature of the height curves of the outer and inner rail heights decreases almost twofold, and its opposite signs rule out the impact of such curvature on accelerations impacting the vertical railway vehicle axis. Given these conditions, the function values $d\psi/dt$ at each relative coordinate $\delta_b \le \delta \le \delta_e$ of the TS length can be calculated by the formula

$$\frac{d\psi}{dt} = v^2\left(\frac{d^2k_H}{dl^2}v^2 - g\frac{d^2i}{dl^2}\right) \quad (14),$$

where

k_H is the function of the curvature trajectory of the railway vehicle reference point at the designed level *H*

[0026] The *L, Z, U* values, as well as predetermined *V, R, D, H,* and *S*, values are a part of the equations of functions

that are equations of functions that are part of the functionality (14). This enables a targeted search for the best possible combination of the *L, Z, U* values, whereby the dispersions *W* of the oscillation amplitude, calculated by the formula (13), will tend to zero. Subject to the foregoing substantiations, this is set to provide the highest quality of the curvilinear railway vehicle motion, evaluated at COM or at any other railway vehicle level that is functionally relevant.

[0027] TS shape reliability and harmonization quality tests revealed that at the design USA values $a_{max} \geq 0.4$ m/s^2 the minimized dispersion of the oscillation amplitudes of the functionality values $d\psi/dt$ needs to be assessed within the diagram $\psi(l)$ "plateau", which is confined to the points with relative TS percentages δ_b = 1/4 and δ_e = 3/4. For USA values within the $0.1 \leq a_{max} < 0.4$ m/s^2 range, such relative boundary percentages have to be calculated using the empirical formulas

$$\delta_b = \frac{1}{4} - \frac{2}{10}\left(3\left(\frac{0.4 - a_{\max}}{0.35}\right)^2 - 2\left(\frac{0.4 - a_{\max}}{0.35}\right)^3\right) \quad (15),$$

$$\delta_e = \frac{3}{4} + \frac{2}{10}\left(3\left(\frac{0.4 - a_{\max}}{0.35}\right)^2 - 2\left(\frac{0.4 - a_{\max}}{0.35}\right)^3\right) \quad (16).$$

[0028] The test in question revealed that the curves that ensure the so-called balanced mode of railway vehicle travel at $|a_{max}| \leq 0.1$ m/s^2, call for substantially longer TS lengths [7]. This said, the expediency of hands-on deployment of such curve configuration is highly dubious and in a number of cases not feasible. Primarily due to the turning radius constraints or for other reasons. Therefore, the minimum design USA value a_{max}, at which it is advisable to harmonize the TS shape, needs to be less than 0.1 m/s^2.

[0029] The TS shape is harmonizable through "manual" selection of combinations that are close to the optimal *L, Z,* and *U* values. However, it should be borne in mind that for program-based harmonization of TS shapes using mathematically substantiated methods, the functional minimum (13) varied within the $1.0E\text{-}7 \leq W \leq 1.0E\text{-}4$ m/s^4 range. The foregoing *W* values hold true for the design railway vehicle speed, varying within the $100 \leq V \leq 400$ km/hr range, curve radii *R*, ensuring design USA values a_{max} within the range $0.1 \leq a_{max} \leq 1.0$ m/s^2 with the design cant varying within the $25 \leq D \leq 150$ mm range, and the design railway vehicle level being *H* = 2200 mm, and gauge *S* = 1520 mm. Under different conditions, the variation ranges of the functional minimum (13) can be different.

[0030] However, even for "manual" harmonization of the TS shapes, it is highly recommended that routine calculations and construction of distribution diagrams that allow to control the efficiency of the process and quality of its outcomes, be automated. Ideally, each step of *L, Z,* or *U* revision should result in the minimization of the numeric values of the target function (13), and cause the USA curve $a(l)$ and the curve "plateau" section $\psi(l)$ to become more straight. In working on the present invention, Microsoft Excel proved itself a rather useful and helpful tool. Alongside with the numeric assessment of the extent of the TS shape harmonization, its quality was corroborated by the diagrams showcasing the geometric and functional properties of the TRV system. The same software was used to calculate the coordinates and other parameters required to break down curves with harmonized TS shapes in line with the respective provisions hereof.

[0031] Thus, the preferred shapes of embodiment of the claimed transition section at the set *U* value, varying between -45 and +55, the sum of the base angle functions of the tangent relative to the track axis $\beta_b\left(\frac{l}{L}\right)$, and complements thereto monotonously and continuously varies from 0 to $L/2R$, and its first derivative with respect to the length $\Delta_\beta\left(\frac{l}{L}\right)$, defining the relationship of curvature of the transition section axis *l*, is varies strictly monotonously and continuously from 0 to $1/R$, and for the sum of all subsequent 2nd, 3d, 4th, and 5th derivatives of the same functions with respect to the same length $k\left(\frac{l}{L}\right) = d\left(\beta_b\left(\frac{l}{L}\right) + \Delta_\beta\left(\frac{l}{L}\right)\right)\Big/dl$ ensures continuity of changes of their values, and renders them equal at both ends of the interval *l*. Track axis curve function $k(\chi)$ is in this case determined using the above formulas (10) - (12). !!!!

[0032] Preferred embodiments include the claimed transition section, wherein, with a specified value of the Z parameter,

varying in the range of -88 to +33, the sum of the functions of the main track transverse inclination $i_b\left(\frac{l}{L}\right)$ and the additions thereto $\Delta_i\left(\frac{l}{L}\right)$ along the entire length *L* of the transition section varies in a consistent monotonous manner in the range of 0 to *D*/*S,* and the values of its 1st, 2nd and 3rd derivatives along the length *l* constantly vary, provided that they equal to zero at both interval ends $0 \le l \le L$.

[0033] It should be mentioned, that to apply the claimed invention in state-of-the-art computer-aided railway design technologies, software harmonization of TS shapes with the use of the Newton's numerical method is more effective. The key points of the algorithm required to do this and its results, illustrating the advantages of the claimed track curve transition section, will be discussed further in more detail and exemplified by, but not limited to, certain preferred embodiments with reference to the positions in the figures, providing schematic representation of the following:

Fig. 1 - rail track curve plan;
Fig. 2 - patterns for calculating the effects produced by gravitational accelerations (G) at the TOR of rail curves;
Fig. 3 - patterns for calculating the effects produced by centrifugal accelerations (*C*) at the TOR of rail curves;
Fig. 4 - gravitational components of accelerations and interaction forces of TVR system elements;
Fig. 5 - centrifugal components of accelerations and interaction forces of TVR system elements;
Fig. 6, Fig. 7 - sum vectors of rail response forces F_L and F_R, determined with account to the direction of the USA vector a_{max} and F_C force;
Fig. 8 - coordinate method for describing the kinematics of the railway vehicle design point *M*, given the TS geometry;
Fig. 9 - normalized graphs of the *Order (3, 7)* function and its derivatives;
Fig. 10 - curvature $k(l)$ graphs of the track axis and movement trajectories $k_H(l)$ of the rated points;
Fig. 11 - graphs of unbalanced lateral accelerations $a(l)$ acting at different design railway vehicle levels *H*;
Fig. 12 - graphs of the variation rates of unbalanced lateral accelerations $a(l)$ $\psi = da/dt$;
Fig. 13 - graphs of rail response forces and their differences;
Fig. 14 - cross section of the TS track for symmetric superelevation offset *D*;
Fig. 15 - diagrams of rail elevations above the longitudinal TS axis profile for symmetric superelevation offset *D*;
Fig. 16 - cross section of the TS track for asymmetric superelevation offset *D*;
Fig. 17 - diagrams of outer rail elevations and the resulting TS axis elevations above inner rail design profile for asymmetric superelevation offset *D*;
Fig. 18 - design diagram of a unified method for calculating the rectangular coordinates of the TS track axis *n* th point in the local curve tangent system;
Fig. 19 - visualization of the process for minimizing the target harmonized TS shape function in accordance with the invention;
Fig. 20, Fig. 24 - example of the geometry and functionality of the TVR system provided by the harmonized TVR shape according to the invention;
Fig. 25 - example of the dependence of optimal lengths *L* of harmonized TS shapes on the USA a_{max} of design speed *V* and elevations *D,* as well as the dependence of minimum lengths *L* of clothoid and recommended [4] *half-sine* TS shapes on the similar *V* speed with *D* = 150 mm, and the permissible wheel lifting speed along the outer rail elevation $\lambda = 1/10$ km/h.
Fig. 26 - example of a speed *V*-invariant dependence of maximum values ψ_{MAX} of the harmonized TS shapes on USA a_{max} and elevations *D*
Fig. 27 - example of a speed *V*-invariant dependence of shifts *p* of the circular axis curves of harmonized TS shapes on USA a_{max} and elevations *D*

[0034] The rail track plan consists of an alternating sequence of straights 1 and curves fitting into their turning angles. Each curve (schematically shown in Fig. 1) consists of two transition sections (TS) 2 and a circular section 3, located in-between them, of the rail track with specified curvature $K = 1/R$. With a known track width *S,* the radius of its axis *R* is consistent with the rated values: railway vehicle movement speed *V*, outer above inner rail elevation *D*, and USA a_{max}, acting at the TOR level. TS 2 axis is designated by number 4.

[0035] Fig. 2 and Fig. 3 show patterns for calculating the effects produced by gravitational accelerations *(G)* and

centrifugal accelerations *(C)* acting on the railway vehicle at the TOR level of the track curve. These patterns correspond to conventional formulas that evaluate the action of gravitational acceleration vector $G = 9.81$ m/s^2 (Fig. 2) and centrifugal acceleration vector $C = k \cdot v^2$ m/s^2 (Fig. 3) at track curves of constant or variable curvature, without taking account of the elevation of the railway vehicle mass center or the vestibular apparatus of the passengers above the TOR level. Fig. 3 shows the outer rail designated by position 5, hereinafter also referred to as the "left" rail, and the inner rail designated by position 6, hereinafter also referred to as the "right" rail.

[0036] Fig. 4 schematically shows acceleration vectors G_L and G_R acting normal to the wheelset axis of the railway vehicle 7, the values whereof depend on the gravitational acceleration g = 9.81 m/s^2, the angle α of the track transverse inclination *i*, and the parameter *H* to S ratio, as well as on the vertical accelerations resulting from the movement speed *V*, the vertical axis curvature k_V, as well as the curvature k_L and k_R of the diagrams describing the superelevation offset *D* of the track's left and right rails (gravitational components).

[0037] Fig. 5 schematically shows a graphical representation of acceleration vectors C_L and C_R acting normal to the wheelset axis, the values whereof depend on the curvature of the rated railway vehicle point trajectory 7 and movement speed *V*, as well as on angle α of the track transverse inclination *i* and the parameter *H* to S ratio (centrifugal components).

[0038] Fig. 6, Fig. 7 schematically show the sum vectors of response force F_L of the left 5 (outer) rail and the response force F_R of the right 6 (inner) rail, determined with account to the direction of the USA vector a_{max}, as well as the resulting centripetal or centrifugal direction of the transverse response force vector F_C of the left (outer) or right (inner) rail.

[0039] Fig. 8 shows a calculation pattern to take account of the TS track shape geometry, as well as the elevation *H* at *M* point above the TOR level using the coordinate method in describing its kinematics.

[0040] Fig. 9 - Fig. 13 schematically shows graphs of normalized geometry of function *Order (3,7) [3]* that is the closest to the TS shape claimed herein, as well as the inherent oscillation amplitudes of integrative performance indicators of the TVR system, that are represented by the graphs of its track axis curvature and of rated points movement trajectories at different railway vehicle levels (Fig. 10), USA *a*(*l*) (Fig. 11), and their variation speed *daldt* (Fig. 12), acting at the same railway vehicle levels, as well as the response forces of the left F_L, and right F_R rails and their differences (Fig. 13). All the indicators used as the basis to plot these graphs were calculated using MDKM dependencies [6] at *V* = 400 km/h, *R* = 8000 m, *D* = 150 mm, *S* = 1520 mm, and *L* = 420 m at design level *H* = 2200 mm.

[0041] Fig. 14 schematically shows the TS track cross-section and the corresponding *half-sine* relationships shown in the diagrams describing the elevations of rail heads above the TS line, that is longitudinal to the axis profiles, for their symmetric superelevation offset by the value of $\pm D/2$ (see Fig. 15).

[0042] Fig. 16 schematically shows the TS track cross section and the corresponding *half-sine* relationship shown in the diagram describing the elevations of the outer (left) rail head above the longitudinal top line of the inner (right) rail head for its asymmetric superelevation offset by the value of *D*, as well as the relationship shown in the diagram describing additional track axis elevations above the design position (see position 8), conditioned by this offset method (see Fig. 17).

[0043] Fig. 18 shows a calculation pattern of a unified method for calculating local rectangular coordinates *of* the *n*-th point of the TS track axis of any shape with a known tangent angle function with respect to it $\beta(\delta)$. The drawing positions indicate axis 9 of the straight track section, axis 4 of the track curve transition section, and axis 10 of the track curve circular section of radius R.

[0044] Fig. 19 provides a graphical representation and analytics of the target TS shape harmonization function, the geometry whereof is described by common relationships (formulas) (1) - (12). The dotted lines demonstrate the relationships shown in the diagrams describing values $d\psi/dt$ of function (14) and their oscillations, the variance whereof in amplitudes consistently decreases in the course of harmonization.

[0045] Fig. 20 - Fig. 24 provides a graphical example of the TVR system geometry and functionality provided by the harmonized TVR shape according to the invention (in one of the possible, but not limiting, embodiments) with optimal values of *L* = 420 m, *Z* = 0.64, *U* = -0.38, and the specified values of parameters *V* = 400 km/h, *R* = 8000 m, *D* = 150 mm, *S* = 1520 mm, and *H* = 2200 mm.

[0046] Fig. 25 shows the dependences of the optimal TS lengths *L* of the track curve *S* = 1520 mm on USA a_{max}, obtained through their harmonization with fixed the values of *H* = 2200 mm for 240 combinations of sampled values of predefined parameters *V, R,* and *D*. This sample included 4 discrete speeds varying in steps of 100 km/h in the range of $100 \le V \le 400$ km/h, for each of which 6 discrete values of the outer rail elevation above the inner one were set, varying in steps of 25 mm in the range of $25 \le D \le 150$ mm. For each of the so generated 24 options for combining different values of *V* and *D* pairs, 10 radii *R* were calculated, providing the corresponding number of discrete USA values a_{max}, varied in steps of 0.1 m/s^2 in the range of $0.1 \le a_{max} \le 1.0$ m/s^2. When displaying points with a_{max} coordinates, the X axis scale and the range of optimal lengths *L* displayed thereon for each of the 3 speeds, V = 300 km/h, V = 200 km/h, and V = 100 km/h, were consistent with the optimal horizontal lengths L, calculated at the design speed of V = 400 km/h. As a result, the position of all 180 points with the same ordinates a_{max} and different abscissas *L,* calculated at the design speeds of *V* = 300 km/h, *V* = 200 km/h, and *V* = 100 km/h, coincided with the position of 60 points with the same ordinates a_{max} and abscissas *L*, calculated at the design speed of *V* = 400 km/h. This made it possible to present the TS shape harmonization results, obtained over the entire scope of the sample, with the use of only 6 lines of a single

graph of hypothetically exponential dependences of optimal TS lengths *L* on a subset of options for combining the values of parameters *V, R, D, H,* and *S*, where radius *R* in each of the options is consistent with the *V, D,* and *S* parameters according to the calculated USA curve value a_{max}, varied in the range of $0.1 \le a_{max} \le 1.0$ m/s^2.

[0047] Likewise, Fig. 25 shows a vertical line of a graph that traditionally limits minimum lengths *L* of clothoid TS shapes according to the maximum permissible wheel lifting speed of $\lambda = 1/10$ km/h. Also, Fig. 25 shows graph lines that limit the minimum lengths of some *half-sine* TS shapes with the same parameters *V, R,* and *D* = 150 mm. These lengths take account of the coefficients recommended in [4]. With these parameters, the optimal lengths of the harmonized TS shapes coincide with the minimum lengths of clothoid and *half-sine* TS shapes only for one of the USA values a_{max}, varied in this case in the range of $0.1 \le a_{max} \le 0.3$ m/s^2. These lengths differ significantly for other calculated USA a_{max} values. It is quite obvious that the variation of the acceptable wheel lifting speed permitted in different countries in the range of $\frac{1}{10} \le \lambda \le \frac{3}{10}$ [4, 8, 9, 10] will not eliminate the fundamental differences in the dependencies presented in Fig. 25. Therefore, the provisions describing practical embodiments of the present invention provide for the harmonized TS shape design only with optimal lengths *L* corresponding to their parameters.

[0048] Fig. 26 - 27 provide examples of dependences of the maximum values ψ_{max} (Fig. 26) and shifts *p* of the circular curve axes sections (Fig. 27) on the rated USA a_{max} and elevations D, corresponding to the optimal values of the L, Z, and U parameters of the same 240 harmonized TS shapes according to the invention (in one of the possible, but not limiting, embodiments), taken into account in the graphs in Fig. 25. As opposed to the graphs of optimal lengths *L* dependences shown in Fig. 25, dependences of maximum values ψ_{MAX} (Fig. 26) and shifts *p* of circular axes curves (Fig. 27) are invariant to the calculated speed *V* in this representation form.

[0049] The geometry of the proposed TS track curve is determined, and the claimed TS operates as follows.

[0050] Each track curve consists of a circular section 3 and two transition sections (TS) 2 connecting it with respective straight sections 1. Axis 4 of the circular track section is circumscribed by an arc of a given curvature K = *1*/*R*. With a known track width *S,* its radius *R* is assigned depending on the rated values: railway vehicle movement speed *V*, elevation *D of* outer rail 5 above inner rail 6 and USA a_{max} acting at a functionally relevant level of design railway vehicle *H*. In accordance with the calculation pattern shown in Fig. 8 for the kinematic model [6], the curvature radius of the horizontal projection of point *M* trajectory, elevated above the TOR by the value of *H,* R differs from it by a very small fraction $H\frac{D}{S}$ on a circular trajectory section with a constant track axis curve radius. Therefore, the maximum USA value a_{max} on a circular track section is calculated with the accuracy sufficient for practical purposes, using the following formula

$$a_{max} \approx K \cdot v^2 - g \cdot \frac{D}{S} \qquad (17),$$

[0051] With a fixed value of design speed *V*, the required balance of constant values $a_{max} \le a_{\partial on}$ at this curve section is achieved by selecting the required combination of *R* and *D* values, acceptable under the design conditions.

[0052] In contrast, the shape of the claimed TS track curve preceding the circular section is determined subject to a functional and two geometric requirements:

- monotonous and smooth variation in the track transverse inclination *i*(*l*) and the axis curvature *k*(*l*) must be observed over the section where these parameters vary from zero on the straight track section to maximum values on the circular curve section;
- the TS shape geometry must be in line with the beam flexural theory on elastic foundation;
- the length and bending patterns of the TS rail curve in the horizontal and vertical projection plane must be aligned in order to provide a perfectly functioning TVR system.

[0053] The required geometry is achieved due to the claimed properties of the track axis arc angle variation functions, the track curvature, and the transverse inclination. The rail bending they describe ensures G^{3rd} order of geometric smoothness in the vertical projection plane, and G^{6th} order in the horizontal projection plane.

[0054] Compliance with the functional requirement is achieved due to the variability of the claimed properties of non-identical track axis curve variation functions and the track transverse inclination. Variation in the TS length and shape affects the kinematics of the rated point at a functionally relevant railway vehicle level, elevated above the TOR by the value of $H > 0$. Integrative quality indicators of this process are incorporated into the formalized goal of the procedure used to agree the values of the controlled and preset parameters of the TVR system, securing the maximized performance

of their interaction. This goal is achieved with optimal values of controlled parameters *L, Z,* and *U,* calculated for the specified values of the *V, R, D, H,* and S parameters in the following sequence.

1. Given the USA a_{max} calculated by formula (17), formulas (15) and (16) are used to calculate the corresponding relative portions δ_b and δ_e of the functional diagram section length (14), within which the variance in oscillation amplitudes *W* of its values must be evaluated and minimized in line with the target function (13).
2. Initial values of the required parameters are set: *L* = 20 m, *Z* = 0, and *U* = 0.
3. The optimal values of these parameters are approximated in 5 cycles. Within such cycles, 20 Newton iterations are run to first sequentially approximate the *L* value with the fixed current values of *Z* and *U*, the value of *Z* is then approximated with the fixed current values of *L* and *U,* and finally the value of *U* is approximated with the fixed current values of *L* and Z. Meanwhile:

- new values of each parameter, set at the end of each 20th iteration cycle of approximation, which will be subsequently taken into account in the approximation of further parameters, are selected from the list of their correct values ensuring the lowest variance of *W* in line with condition (13);
- function (14) $d\psi/dt$ values required to calculate *W,* and its partial derivatives should be calculated in steps of $\Delta\delta = (\delta e - \delta_b)/(M - 1)$ with $M \geq 1000$;
- the results will be incorrect in the following cases:

  - the *L* length is negative or exceeds the permissible length for a given curve;
  - during the calculations, *Z* values go beyond the permissible range of $-88 \leq Z \leq 33$;
  - during the calculations, *U* values go beyond the permissible range of $-45 \leq U \leq 55$;

- curvature k_H of the railway vehicle rated point trajectory at level *H,* as well as its derivatives required to calculate the current values of function (14), should be calculated taking into account the deterministic MDKM dependencies described in [6];
- each of the parameters L_{n+1}, Z_{n+1}, and U_{n+1} claiming to be a new approximate value is calculated using the following formulas

$$L_{n+1} = L_n - \sum_{\delta=\delta_b}^{\delta=\delta_e} \left(\frac{d\psi(\delta)}{dt} \right)^2 \Bigg/ \left(6 \cdot \sum_{\delta=\delta_b}^{\delta=\delta_e} \frac{d\psi(\delta)}{dt} \cdot \frac{\partial^2 \psi(\delta)}{\partial t \partial L_n} \right) \quad (18),$$

$$Z_{n+1} = Z_n - \sum_{\delta=\delta_b}^{\delta=\delta_e} \left(\frac{d\psi(\delta)}{dt} \right)^2 \Bigg/ \left(6 \cdot \sum_{\delta=\delta_b}^{\delta=\delta_e} \frac{d\psi(\delta)}{dt} \cdot \frac{\partial^2 \psi(\delta)}{\partial t \partial Z_n} \right) \quad (19),$$

$$U_{n+1} = U_n - \sum_{\delta=\delta_b}^{\delta=\delta_e} \left(\frac{d\psi(\delta)}{dt} \right)^2 \Bigg/ \left(6 \cdot \sum_{\delta=\delta_b}^{\delta=\delta_e} \frac{d\psi(\delta)}{dt} \cdot \frac{\partial^2 \psi(\delta)}{\partial t \partial U_n} \right) \quad (20)$$

- following these recommendations will help minimize target function (13) with $W \leq 1.0E-03$ or with a much better result.

4. The TS *L* length, so calculated, is rounded to the nearest larger integer value, that is a multiple of 1 m. Any coarser rounding, for example, a multiple of 5, 10 or up to 20 or more meters, is extremely undesirable. Especially, it concerns any rounding to a smaller value, for it causes a significant increase in the variance in function $d\psi/dt$ oscillation amplitudes. Ultimately, this can lead to vibration, shocks or rocking of the railway vehicle body during the TS operation at the design values of the *V, R, D, H,* and S parameters.
5. The values of *Z* and *U* parameters can be rounded with an error of ± 0.01.

[0055] The values of L, Z and U parameters that are consistent with these requirements are harmonized with the values of other preset track curve and design railway vehicle parameters V, R, D, H, and S. They will be relevant and may be used multiple times in constructing a TS of the claimed shape in other track curves with a similar or different

rotation angle $\pm\theta$ subject to the condition of $|\theta| \geq L/R$ and provided that the calculated values of preset parameters *V, R, D, H,* and *S* are constant. In case of a change in at least one of the said parameters, repeat the calculations of the parameters *L, Z,* and *U* per paragraphs 1 through 5 of the above harmonization procedure.

[0056] With the current values of parameters *L, Z,* and *U,* the relative rectangular coordinates *x*[*n*] and *y*[*n*] of the claimed TS axis should be calculated using formulas (1) and (2) where $N = L*10 + 1$. Subject to this condition, the difference between the arc length $\Delta_l = 0.1$ m and the length of the relevant contracting chord from point *n* -1 to point *n* will be immaterial. This will provide the sufficient detail and accuracy for practical purposes in the calculations of both the absolute coordinates of the curve axis of a system installed in the unit, and its other geometry. In this case, the values of tangents, bisectors, center of the circular curve, and its displacement, that are necessary for the track curve configuration with a TS of the shape claimed herein, are calculated with the use of standard methods and well-known formulas applicable to the curve with any other TS shape with known local coordinates *x*[*N* -1] and *y*[*N* -1] of the point at the end of the track axis for each TS and angle β of the entire arc of its axis.

[0057] Using the traditional technology of point-by-point in-situ marking of the claimed shape TS axis with a step greater than Δ_l, one can use the coordinates of only those points, the multiplicity of whose numbers is in line with these requirements. When constructing a TS track of the claimed shape with the use of automated control systems for track renewal trains, as well as when building their 3D models with the use of cutting-edge information technologies, it is advisable to determine the location of the TS track axis with a decimeter step that provides a sufficient level of detail. To do this, one should take into account the coordinates of all N points calculated using formulas (1) and (2).

[0058] The design and functional advantages offered by the TS track curve of the shape claimed herein were confirmed by the harmonization of 240 combinations of preset track curve parameters, with a track width of $S = 1520$ mm, generated at 4 discrete speeds *V*, varied in increments of 100 km/h in the range of $100 \leq V \leq 400$ km/h, while for each of them 6 discrete values of the outer rail elevation over the inner one were set, that were varied in increments of 25 mm in the range of $25 \leq D \leq 150$ mm. For each of the so generated 24 options of a combination of different *V* and *D* pairs, 10 radii *R* were calculated, providing the corresponding number of discrete USA values a_{max}, varied in steps of 0.1 m/s^2 in the range of $0.1 \leq a_{max} \leq 1.0$ m/s^2.

[0059] The optimal *L, Z,* and *U* values for all 240 options of a combination of *V, R,* and *D* values, with a fixed elevation of the functionally significant level of design railway vehicle $H = 2200$ mm, were calculated at $1.0E\text{-}07 \leq W \leq 4.0E\text{-}04$. Such minimization degree of the target function (13) helped achieve high performance of the TVR system, confirmed by G^1-smooth quasi-linear USA $a(l)$ diagrams (see Fig. 22) and G^0-smooth trapezoidal diagrams of its rate of change $\psi = da/dt$ (see Fig. 23). Also, the deviations of maximum speeds ψ_{max} from the absolute, yet virtually unattainable minimum value ψ_{MIN}, were significantly smaller than those of the known TS shapes of the prior art with similar values of the parameters *V, R, D,* and *L*. Along with the values of the parameter ψ_{max}, the TS shape harmonization data was supplemented with the values of the so-called circular curve displacement *p,* the value whereof, in combination with the values of *R* and *L,* can be used to evaluate the design advantages of the TS shape claimed, that are important for rail road setting.

[0060] Some of the data obtained by harmonizing the TS shapes with design elevation $D = 150$mm for design speeds $V = 400$ km/h, and $V = 100$ km/h are presented in Table 1. Such data suggest of their steady dependence on the USA a_{max} design values. The nature and features of this dependence are illustrated in more detail in the graphs in Fig 25, 26, and 27.

Table 1. Example of optimal *L, Z,* and *U* values of the claimed TS shapes with $D = 150$mm, harmonized for the calculated USA values, varying in the range of $0.1 \leq a_{max} \leq 1.0$ m/s^2 at $V = 400$ km/h (see the numerator) and $V = 100$ km/h (see the denominator) for $H = 2200$mm and $S = 1520$mm

a_{max}, m/s^2	*R*, m	*L*, M	*Z*	*U*	ψ_{MAX}, m/s^3	*p*, m
0.1	12110 / 760	930 / 233	-3.52 / -4.52	6.52 / 8.52	0.014 / 0.014	0.932 / 0.960
0.2	11030 / 690	686 / 171	-0.04 / -0.31	-0.11 / -0.11	0.035 / 0.035	0.561 / 0.558
0.3	10120 / 630	580 / 145	0.43 / 0.25	-0.62 / -0.62	0,063 / 0.063	0.437 / 0.436
0.4	9360 / 585	513 / 128	0.26 / -0.04	-0.15 / -0.32	0,095 / 0.095	0.370 / 0.368
0.5	8700 / 545	464 / 116	0.40 / 0.16	-0.45 / -0.33	0.132 / 0.131	0.325 / 0.325
0.6	8125 / 510	426 /106	0.01 / -0.26	-0.42 / -0.18	0.172 / 0.170	0.294 / 0.295
0.7	7620 / 480	397 / 99	-0.03 / -0.30	-0.18 / -0.22	0.216 / 0.217	0.272 / 0.271
0.8	7180 / 450	373 / 93	0.18 / -0.53	-0.40 / -0.38	0.263 / 0.26	0.255 / 0.253
0.9	6785 / 425	353 / 88	0.31 / -0.20	-0.59 / -0.71	0.313 / 0.314	0.241 / 0.240

(continued)

a_{max}, m/s^2	R, m	L, M	Z	U	ψ_{MAX} , m/s^3	p, m
1.0	6430 / 400	336 / 84	0.34 / 0.28	-0.43 / -0.39	0.366 / 0.366	0.231 / 0.230

[0061] The analysis of the graphs in Fig. 25 suggests that the exponential dependences of optimal lengths L_{opt} of the harmonized TS of the shape claimed herein differ significantly from the vertical line of the graph describing the dependence of minimum lengths L_{min} of clothoid TS shapes, traditionally normalized by the so-called permissible elevation speed of the outer wheel along the elevation $\lambda = V \cdot D/L$. In this example, it limits minimum lengths L_{min} of clothoid TS curve shapes for the calculated elevation of D = 1500mm with the permissible elevation speed of the outer wheel of λ = 1/10 km/h (≈28 mm/s) as recommended in [8, 9, 10]. In case of using the *half-sine* TS shapes, as recommended in [4], their minimum lengths will differ even greater from the optimal lengths of harmonized TS of the claimed shape. Given the obvious tendency towards increasing the proportionality coefficients, correlating with the order of geometric smoothness of the corresponding types of *half-sine* TS shapes, the minimum lengths of more advanced and smoother *half-sine* TS shapes can be even greater. This suggests of clear issues with empirical methods for normalizing TS lengths according to any of the permissible values of the parameter λ or ratio D/L, whose indirect cause-and-effect relationship with integrative movement quality indicators has not been substantiated.

[0062] The analysis of graphs in Fig. 26 suggests that the harmonized TS of the shape claimed herein are characterized by polynomial dependences of the maximum rate of change ψ_{max} on the calculated USA a_{max} values, which, as opposed to the optimal lengths, are invariant with respect to the calculated movement speed V. In this case, the greater the design elevation D is, the higher will be the design movement comfort with a harmonized TS of the shape claimed herein, corresponding to the ψ_{max} parameter. The graph of function ψ_{max} at D = 150 mm suggests that the function values over the entire USA variation range of $0.1 \le a_{max} \le 1.0$ m/s^2 do not even exceed the lower limit of the traditionally recommended normative range of $0.4 \le \psi_{max} \le 0.6$ m/s^3.

[0063] The analysis of the graphs in Fig. 27 demonstrates that displacements p of circular curves with the harmonized TS, that are shaped as claimed herein, are also characterized by the polynomial dependencies, invariant with respect to the calculated movement speed V, on the calculated USA a_{max} figures. At the same time, the displacements p of circular curves with the harmonized TS, that are shaped as claimed herein, are several times smaller than displacements p of circular curves of clothoid TS shapes that are common and problematic. The calculations demonstrate that the multiple difference between such displacements contributes to the reshaping of clothoid TS curves into harmonized ones, that are shaped as claimed herein, in order to achieve a higher speed and ease of movement while facing the lowest requirements as regards straightening of the existing tracks.

[0064] Taking account of the above relationships can help make optimal decisions when constructing new rail road curves or reconstructing the existing ones. Due to a large number of possible combinations of preset *V, R, D, H,* and *S* values varying in a fairly wide range, it is impracticable to provide a traditional presentation of pre-calculated optimal *L, Z,* and *U* values of harmonized TS shapes in tabular form or graphs. Software implementation of the algorithms for harmonizing TS shapes and calculating coordinates necessary for their construction in accordance with this invention is more acceptable for the current computer-aided technologies used in design, construction and operation of railways.

[0065] As opposed to prior art solutions, objective laws of physics and mathematics, and the substantiated harmonization methods underlying this invention help to seek optimal values for all the required design parameters of curve transition sections, the shape geometry of which was described by relationships (1) - (12). They provide the integrative quality of the Track + Railway Vehicle system in a direct and straightforward manner, rather than describing it indirectly. Moreover, this quality depends on the consistency and commensurability of such system parameters as the elevation of railway vehicle's design point *H,* its movement speed *V*, curve radius *R,* outer rail elevation *D,* and the related offset method used. Therefore, the provisions and distinctive features of this invention should also be taken into account at the stage of making decisions as to the basic values of curve parameters in the designed rail tracks.

References.

[0066]

1. Bjorn Kufver, VTI rapport 420A, "Mathematical description of railway alignments and some preliminary comparative studies", Swedish National Road and Transport Research Institute, 1997. Digitala Vetenskapliga Arkivet (digital scientific archive). [Electronic resource] - July 17, 2020. - Access: http://www.diva-portal.org/smash/record.jsf?pid=diva2%3A675179&dswid=4876.

2. Patent EP No. 1523597B1, publ. July 16, 2008

3. Klauder, Louis, T., Jr. Railroad curve transition spiral design method based on control of vehicle banking motion.

Available from: https://patentscope.wipo.int/search/ru/detail.jsf?docId=WO2001098938&recNum=1&maxRec=&office=&prev Filter=&sortOption=&queryString=&tab= PC TDescription
4. EN 13803-1:2010: Railway applications -Track-Track alignment design parameters - Track gauges 1435 mm and wider - Part 1: Plain line [Required by Directive 2008/57/EC]
5. M. Ueno et al.: Motion Sickness Caused by High Curve Speed Railway Vehicles. Jpn J Ind Health 1986; 28: 266-274.
6. Velichko, G. 2020. Quality analysis and evaluation technique of railway track + vehicle system performance at railway transition sections with various shape curves, In Transport Means 2020: Proceedings of the 24th International Scientific Conference, Part 11: 573-578. Available from: https://transportmeans.ktu.edu/wp-content/uploads/sites/307/2018/02/Transport-means-A4-II-dalis.pdf
7. Velichko, G. 2020. Shape Harmonization of the Railway Track Transition Section & the Kinematics of Vehicle Body Design Point, In Transport Means 2020: Proceedings of the 24th International Scientific Conference, Part 11: 910-915. Available from: https://transportmeans.ktu.edu/wp-content/aploads/sites/307/2018/02/Transport-means-A4-II-dalis.pdf
8. G.M. Shakhunyants Railway Track / G.M. Shakhunyants. - Moscow: Transport, 1997. - p. 479
9. Theoretical basis for the introduction of high-speed trains in Ukraine: monograph / M.B. Kurgan, D.M. Kurgan; V. Lazaryan Dnipro National University of Railway Transport - Dnipro, 2016. - p. 283
10. S.V. Shkurnikov et al. General Requirements to the Design of the Moscow-Kazan HSRL "Transport of the Russian Federation" No. 2(57) 2015 p. 26-29

Claims

1. The transition section of the rail track curve, which along the length *L* integrates the adjoining straight section and the circular section of the curve with the constant radius *R,* encompassing the base and track-forming rail-tie grid, resting thereon in full accordance with the coordinates of the projection of transition section points onto a horizontal plane with a variable transverse inclination *i* varying along the length *L* that is normal to the axis line that is tangent to the top of rail, with the track axis shape of the transition section being dependent on the position *N* of equidistant points with the coordinates *x*[*n*] and *y*[*n*], and the transverse inclination *i*[*n*] of the track at such points varying along the transition section axis in the range of $0 \le i[n] \le D/S$, where *D* is the estimated superelevation of the outer rail above the inner one within the rail track curve, and *S* is the distance between the vertical axes of the rail track cross section, as $\Delta_l = L/(N-1)$ the distance *l*[*n*] between each n^{th} point and *l*[0] = 0.0 m increases proportionately by a constant, at the beginning of the transition section axis, and up to *l*[*N* -1] = *L* at the section's end, ***whereby*** the relative rectangular coordinate points of the projected track axis *x*[*n*] and *y*[*n*] have been determined using the formulas:

$$x[0] = 0.0; \qquad x[n] = x[n-1] + \Delta_l \cdot \cos\left(\beta_b(\delta) + \Delta_\beta(\delta)\right) \qquad (1),$$

$$y[0] = 0.0; \qquad y[n] = y[n-1] + \Delta_l \cdot \sin\left(\beta_b(\delta) + \Delta_\beta(\delta)\right) \qquad (2),$$

where:

n is the reference number of the transition section axis point varying within the $1 \le n \le (N-1)$ range,
x[*n*] is the coordinate that characterizes the distance between the start of transition section and location of the n^{th} axis point projected onto a line that is tangent thereto at point *x*[0] and *y*[0],
y[*n*] is a coordinate that characterizes the shift towards the curvature center of the n^{th} axis point normally from the line that is tangent thereto at point *x*[0] and *y*[0],
Δ_l is the transition section length/ track axis complement constant, measured in an arc from its start to each n^{th} point,
δ is the relative percentage of the current length $l + \Delta_l/2$ of the transition section track axis, measured from its start to the middle of the axis section, confined between its adjacent points *n*-1 and *n*, calculated by the formula:

$$\delta = \frac{2n-1}{2(N-1)} \quad (3),$$

$\beta_b(\delta)$ is the value of the base angle function of the tangent to the transition section calculated in accordance with the relative percentage of the δ current length $l + \Delta_l/2$ up to the point of contact, using the formula:

$$\beta_b(\delta) = \frac{L}{R}\delta^6\left(\frac{315}{6} - \delta\left(\frac{2043}{7} - \delta\left(\frac{6720}{8} - \delta\left(\frac{14085}{9} - \delta\left(\frac{19795}{10} - \delta\left(\frac{18579}{11} - \delta\left(\frac{11178}{12} - \delta\left(\frac{3900}{13} - \frac{600}{14}\delta\right)\right)\right)\right)\right)\right)\right)\right) \quad (4),$$

$\Delta_\beta(\delta)$ is the value of the complement base angle function of the tangent to the transition section calculated in accordance with the relative percentage of the δ current length $l + \Delta_l/2$ up to the point of contact, using the formula:

$$\Delta_\beta(\delta) = U\frac{L}{R}\delta^6\left(\frac{7}{6} - \delta\left(\frac{74}{7} - \delta\left(\frac{340}{8} - \delta\left(\frac{885}{9} - \delta\left(\frac{1425}{10} - \delta\left(\frac{1452}{11} - \delta\left(\frac{914}{12} - \delta\left(\frac{325}{13} - \frac{50}{14}\delta\right)\right)\right)\right)\right)\right)\right)\right) \quad (5),$$

where
U is the parameter establishing the base angle complement of the tangent to the transition section axis at its every point with a relative percentage δ of its current length $l + \Delta_l/2$ the transverse inclination $i[n]$ of the transition section track at the n^{th} point of its axis varying within the interval $0 \le n \le (N-1)$ is determined using the formula

$$i[n] = i_b(\chi) + \Delta_i(\chi) \quad (6),$$

where
χ is the relative percentage of the track length/axis to point n, calculated as:

$$\chi = \frac{n}{N-1} \quad (7),$$

$i_b(\chi)$ is the value of the function of the base track transverse inclination of the transition section calculated in accordance with the relative percentage χ, using the formula:

$$i_b(\chi) = \frac{D}{S}\chi^4\left(37 - \chi\left(102 - \chi\left(140 - \chi\left(172 - \chi\left(198 - \chi\left(154 - \chi\left(66 - 12\chi\right)\right)\right)\right)\right)\right)\right) \quad (8),$$

$\Delta_i(\chi)$ is the value of the function of the complement to the track transverse inclination at n, calculated in accordance with the relative percentage χ, using the formula:

$$\Delta_i(\chi) = -Z\frac{D}{S}\chi^4\left(1 - \chi\left(9 - \chi\left(35 - \chi\left(76 - \chi\left(99 - \chi\left(77 - \chi\left(33 - 6\chi\right)\right)\right)\right)\right)\right)\right) \quad (9),$$

where:
Z is the parameter establishing the complement to the primary transverse inclination of the track at its every point n with a relative percentage χ.

2. Transition section according to claim 1, ***whereby*** at the set U value, varying between -45 and +55, the sum of the

base angle functions of the tangent relative to the track axis $\beta_b\left(\frac{l}{L}\right)$, and complements thereto $\chi = l/L$ monotonously and continuously varies from 0 to $L/2R$, and its first derivative with respect to the length $\Delta_\beta\left(\frac{l}{L}\right)$, defining the relationship of curvature of the transition section axis l, is varies strictly monotonously and continuously from 0 to $1/R$, and for the sum of all subsequent 2nd, 3d, 4th, and 5th derivatives of the same functions with respect to the same length $k\left(\frac{l}{L}\right) = d\left(\beta_b\left(\frac{l}{L}\right) + \Delta_\beta\left(\frac{l}{L}\right)\right)\Big/dl$ ensures continuity of changes of their values, and renders them equal at both ends of the interval l, whereby the track curvature function $0 \le l \le L$ where $k(\chi)$ at each current length / TS length is defined as

$$k(\chi) = k_b(\chi) + \Delta_k(\chi) \quad (10),$$

where

$$k_b(\chi) = \frac{L}{R}\chi^5\left(315 - \chi\left(2043 - \chi\left(6720 - \chi\left(14085 - \chi\left(19795 - \chi\left(18579 - \chi\left(11178 - \chi\left(3900 - 600\chi\right)\right)\right)\right)\right)\right)\right)\right) \quad (11),$$

$$\Delta_k(\chi) = U\frac{L}{R}\chi^5\left(7 - \chi\left(74 - \chi\left(340 - \chi\left(885 - \chi\left(1425 - \chi\left(1452 - \chi\left(914 - \chi\left(325 - 50\chi\right)\right)\right)\right)\right)\right)\right)\right) \quad (12),$$

U is a parameter establishing the highest complement to the primary transition section track curvature axis.

3. Transition section according to claim 1, ***whereby*** at the set Z value, varying between -88 and +33, the sum of the base track transverse inclination functions $i_b\left(\frac{l}{L}\right)$, and complements thereto $\Delta_i\left(\frac{l}{L}\right)$ throughout the length L of the transition section is strictly monotonous and continuously varies between 0 and D/S, and the values of its 1st, 2nd, and 3d derivatives with respect to the length l continuously vary as long as they both equal zero at both ends of the interval $0 \le l \le L$.

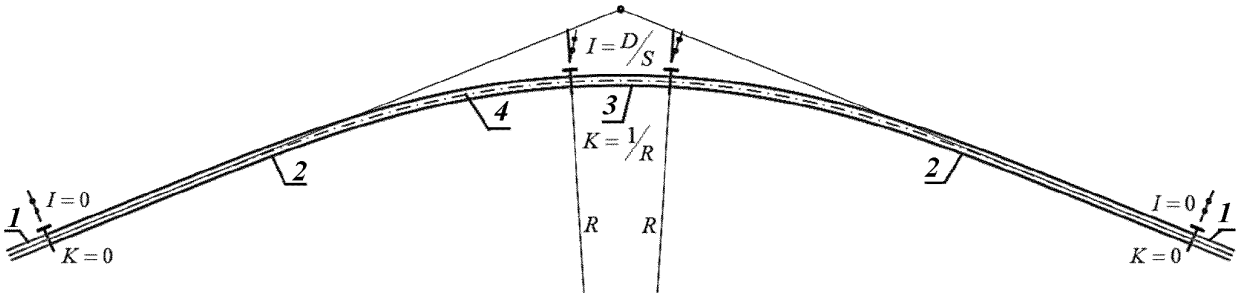

FIG. 1

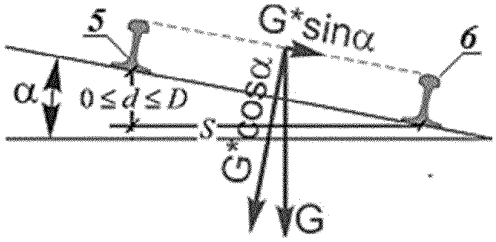

FIG. 2

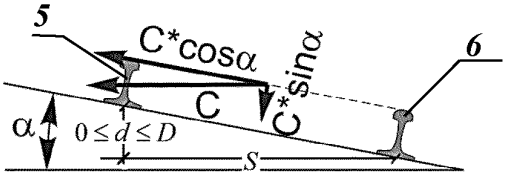

FIG. 3

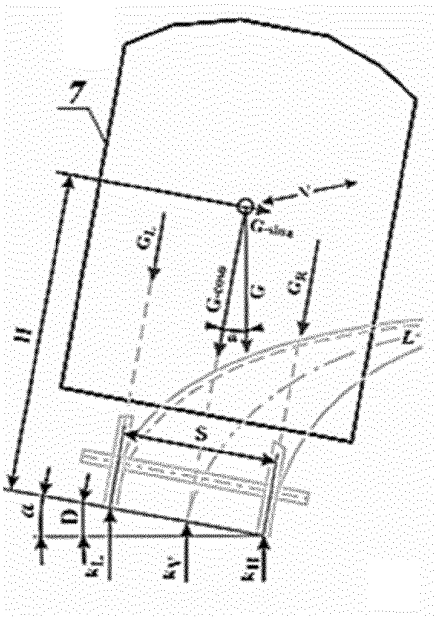

FIG. 4

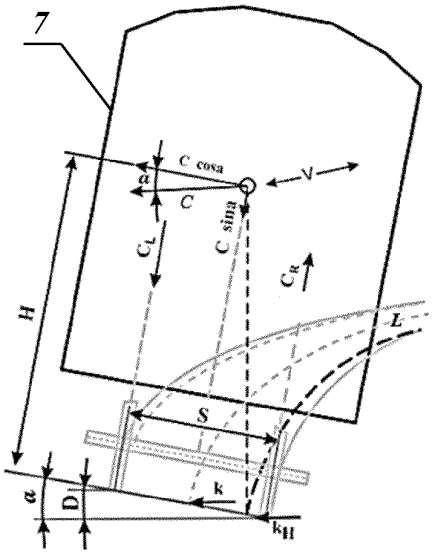

FIG. 5

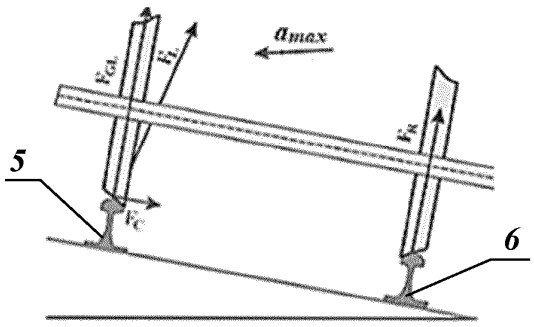

FIG. 6

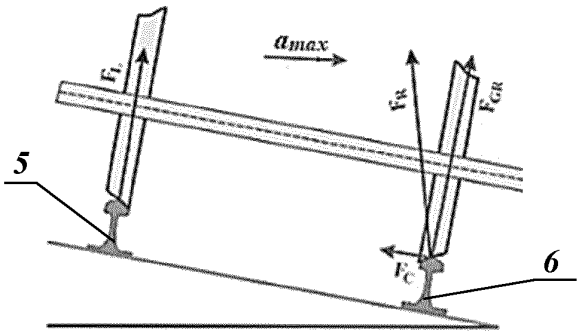

FIG. 7

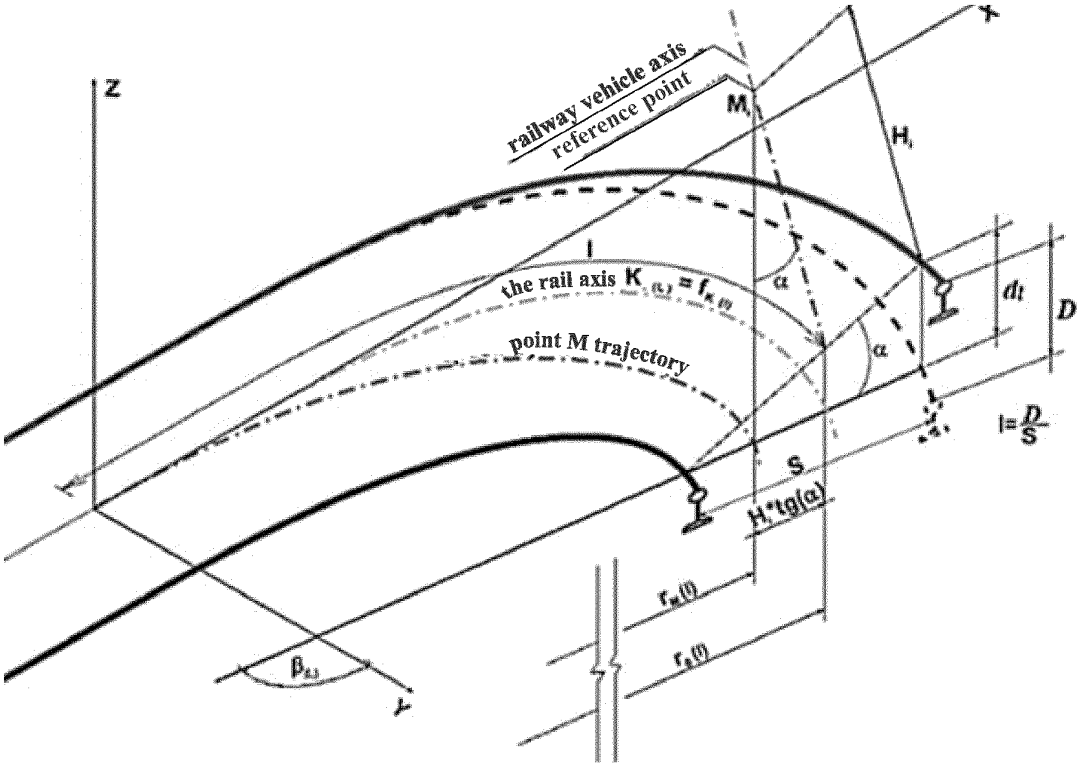

FIG. 8

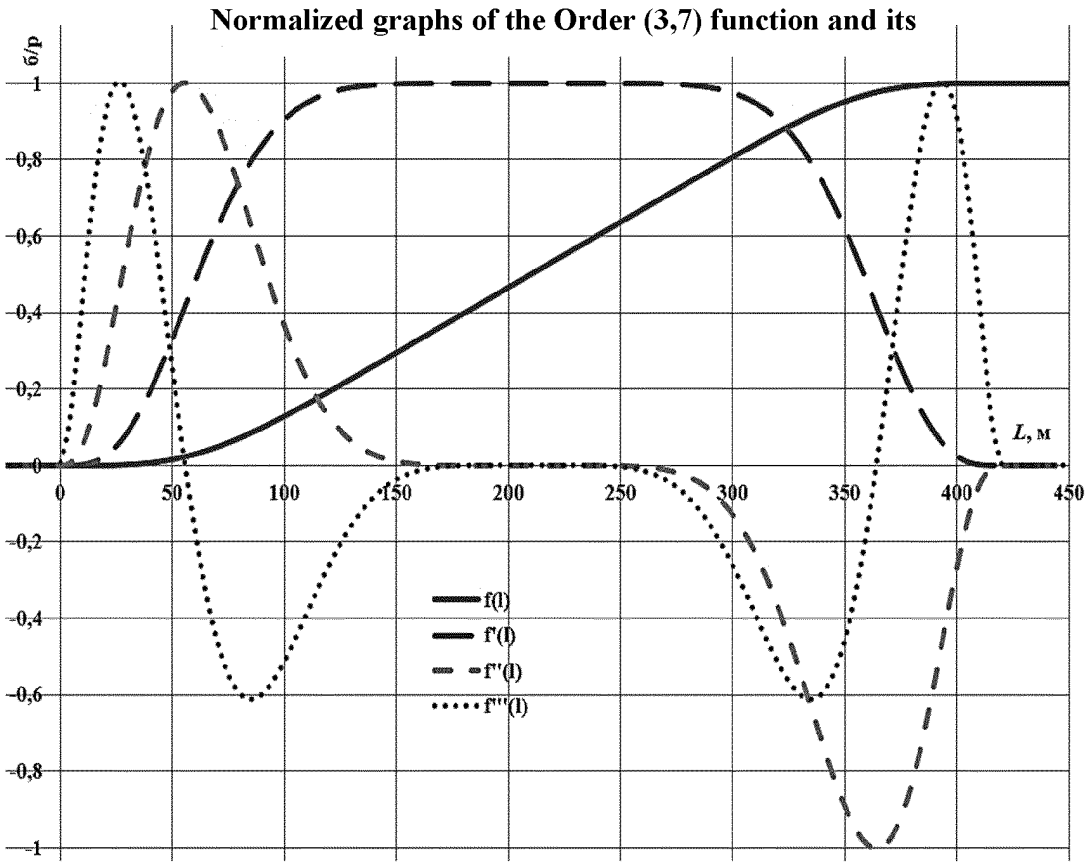
Normalized graphs of the Order (3,7) function and its
6/p
1
0,8
0,6
0,4
0,2
0
-0,2
-0,4
-0,6
-0,8
-1
0
50
100
150
200
250
300
350
400
450
L, м
f(l)
f'(l)
f''(l)
f'''(l)

FIG. 9

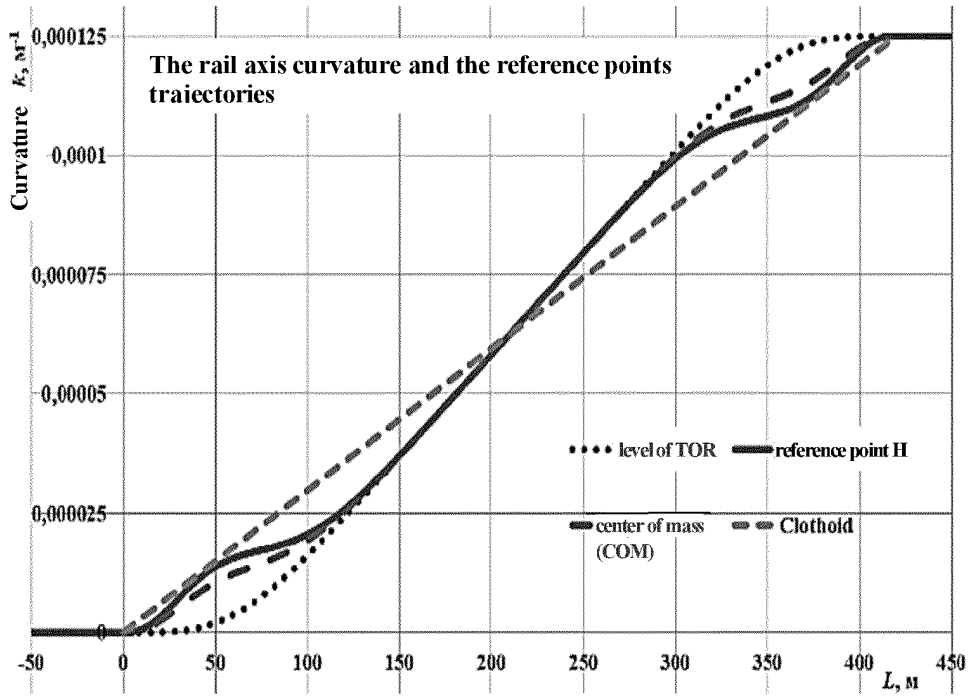
The rail axis curvature and the reference points traiectories
Curvature k, м-1
0,000125
0,0001
0,000075
0,00005
0,000025
0
-50
0
50
100
150
200
250
300
350
400
450
L, м
level of TOR
reference point H
center of mass (COM)
Clothoid

FIG. 10

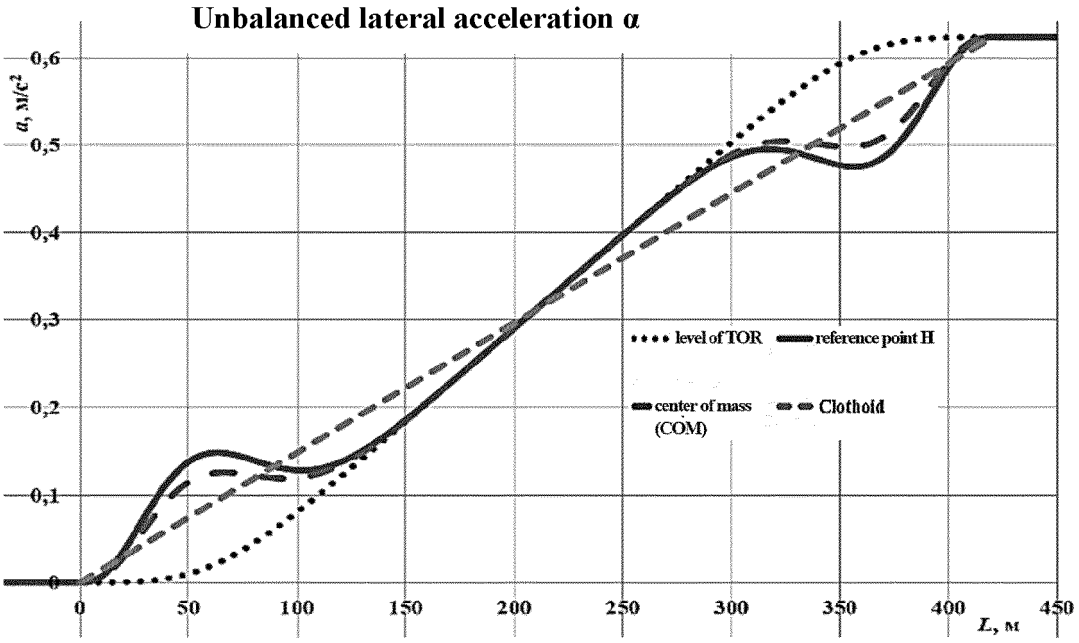
Unbalanced lateral acceleration α
a, м/с²
0,6
0,5
0,4
0,3
0,2
0,1
0
0
50
100
150
200
250
300
350
400
450
L, м
level of TOR
reference point H
center of mass (COM)
Clothoid

FIG. 11

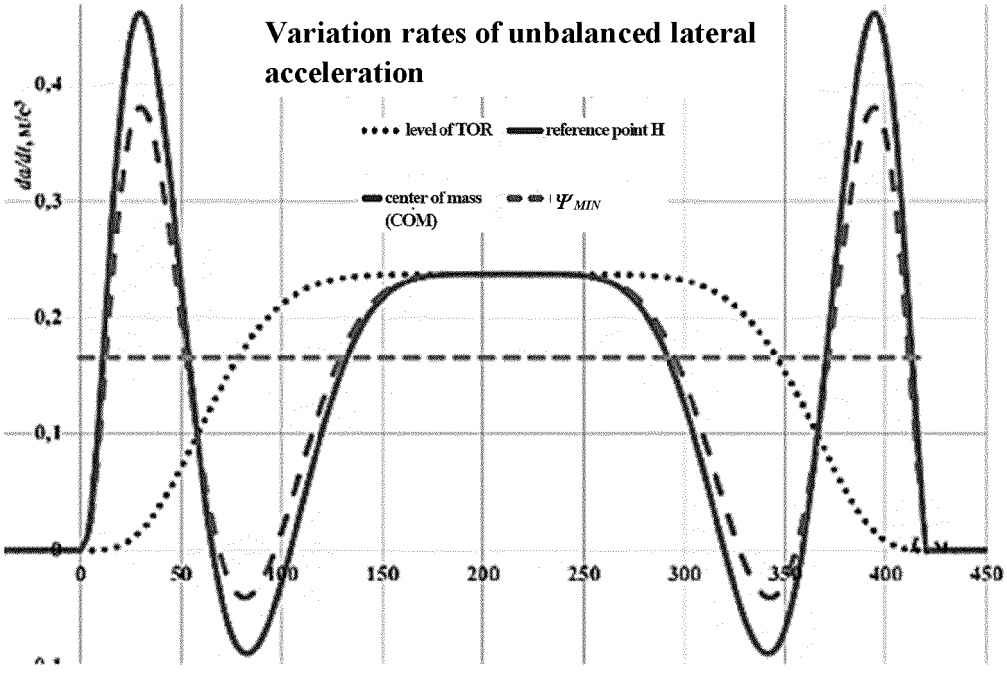
Variation rates of unbalanced lateral acceleration
da/dt, м/с³
0,4
0,3
0,2
0,1
0
0
50
100
150
200
250
300
350
400
450
L, м
level of TOR
reference point H
center of mass (COM)
Ψ_{MIN}

FIG. 12

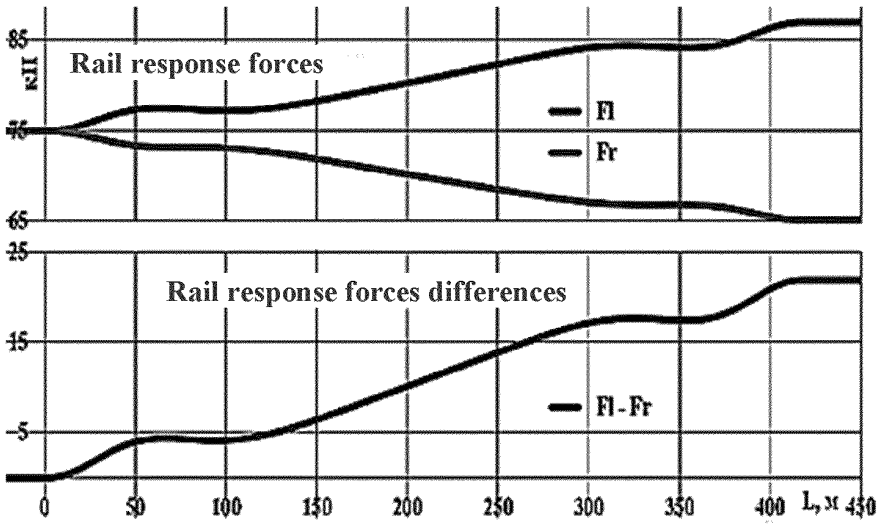

FIG. 13

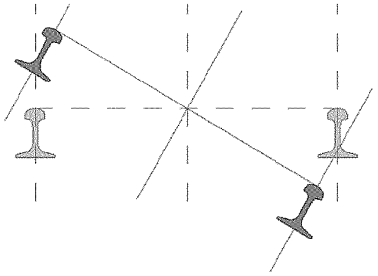

FIG. 14

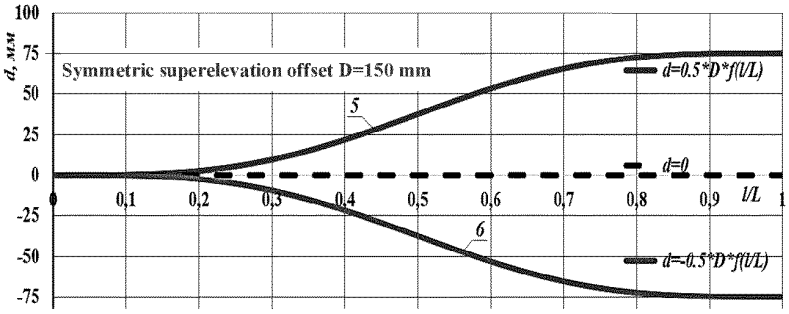

FIG. 15

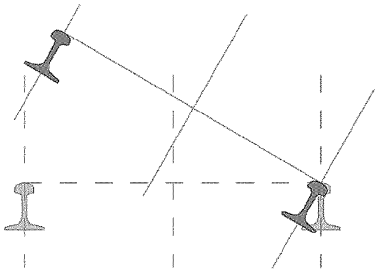

FIG. 16

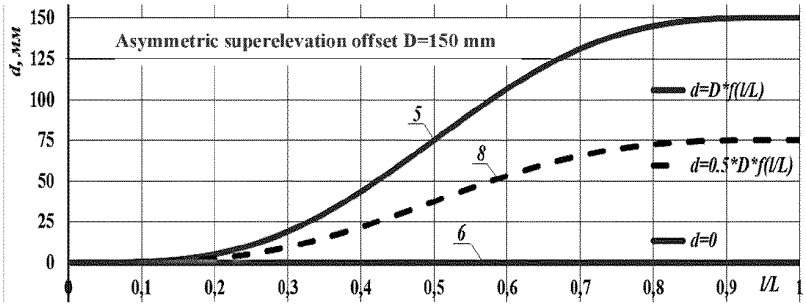

FIG. 17

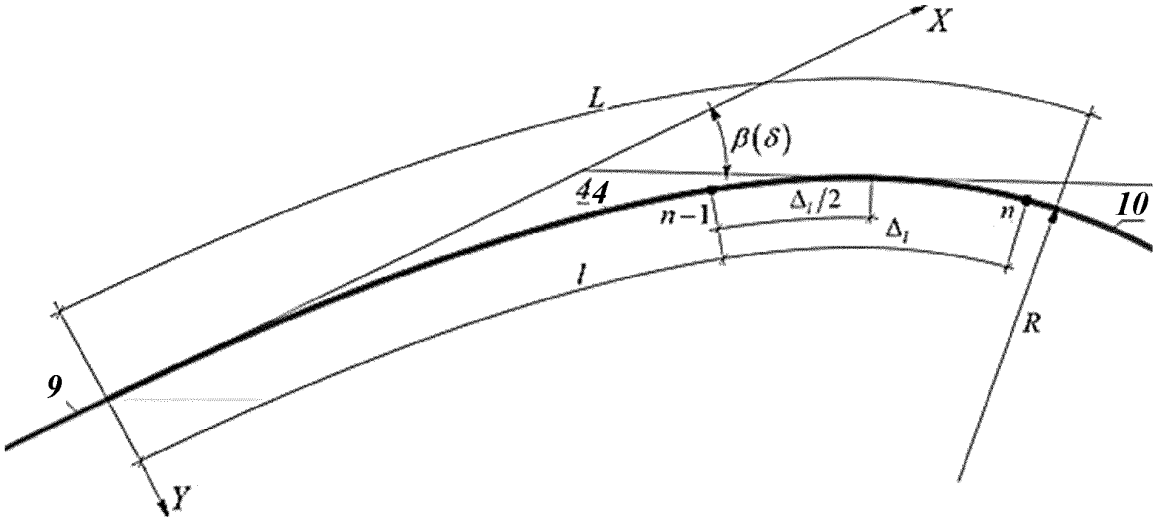
X
L
β(δ)
44
n−1
Δ1/2
Δ1
n
10
l
R
9
Y

FIG. 18

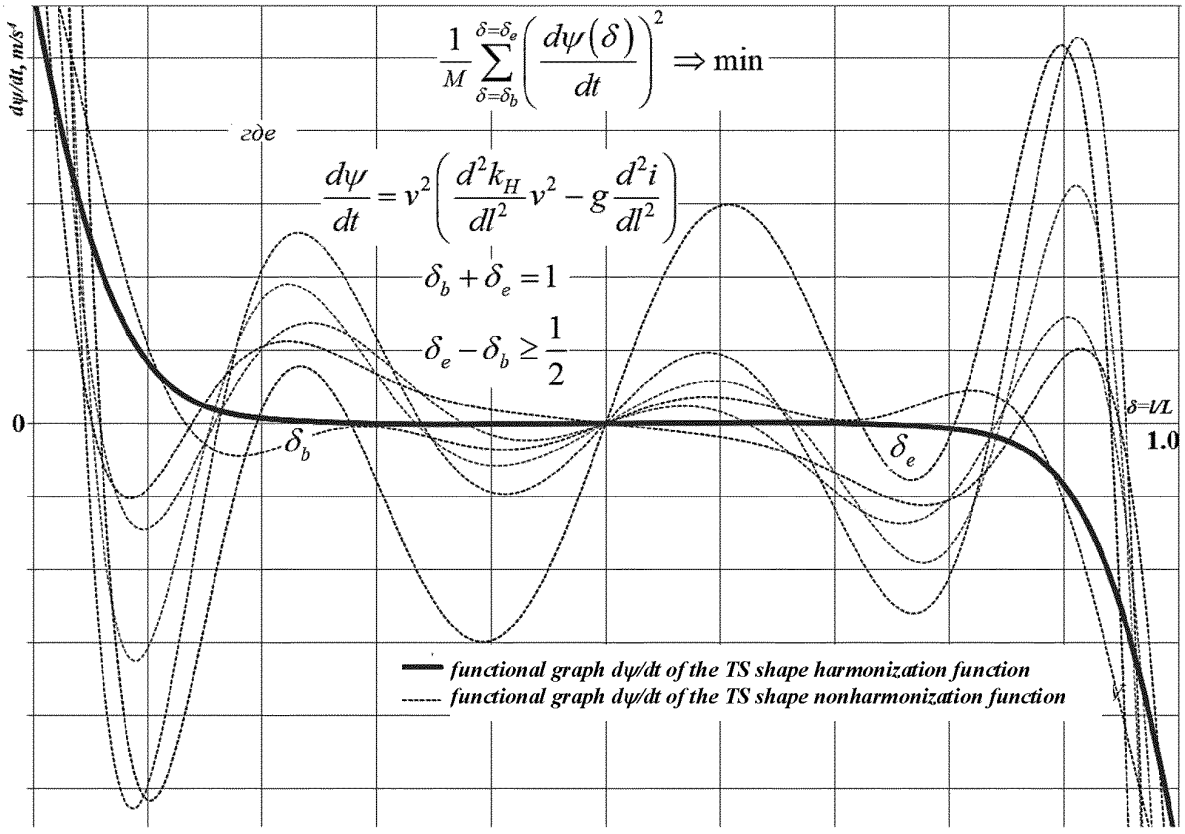
dψ/dt, m/s²
$\frac{1}{M}\sum_{\delta=\delta_b}^{\delta=\delta_e}\left(\frac{d\psi(\delta)}{dt}\right)^2 \Rightarrow \min$
$\frac{d\psi}{dt} = v^2\left(\frac{d^2k_H}{dl^2}v^2 - g\frac{d^2i}{dl^2}\right)$
$\delta_b + \delta_e = 1$
$\delta_e - \delta_b \geq \frac{1}{2}$
0
δ_b
δ_e
δ=l/L
1.0
functional graph dψ/dt of the TS shape harmonization function
functional graph dψ/dt of the TS shape nonharmonization function

FIG. 19

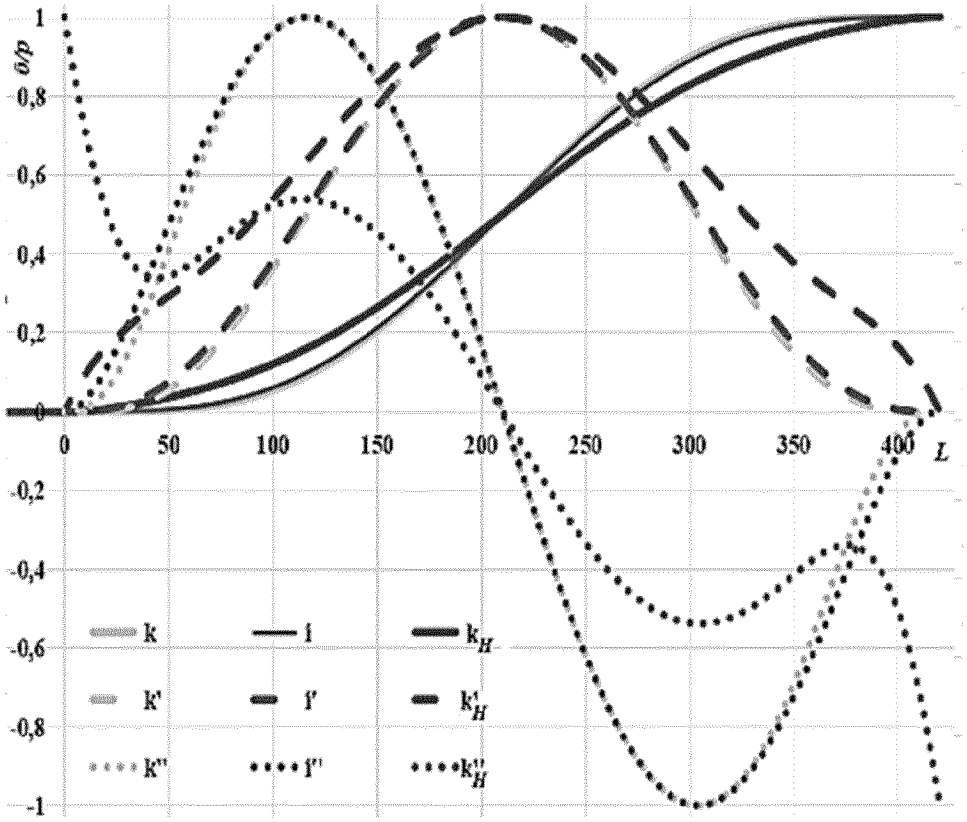
1
0,8
0,6
0,4
0,2
0
-0,2
-0,4
-0,6
-0,8
-1
0
50
100
150
200
250
300
350
400
L
k
l
k_H
k'
l'
k'_H
k''
l''
k''_H

FIG. 20

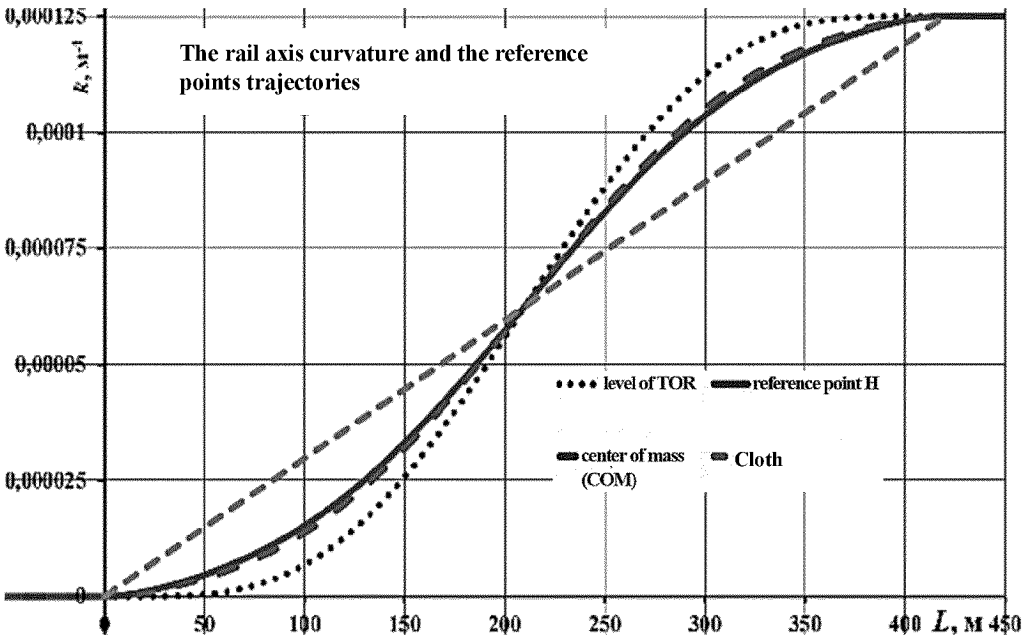
The rail axis curvature and the reference points trajectories
0,000125
0,0001
0,000075
0,00005
0,000025
0
50
100
150
200
250
300
350
400
450
L, м
level of TOR
reference point H
center of mass (COM)
Cloth

FIG. 21

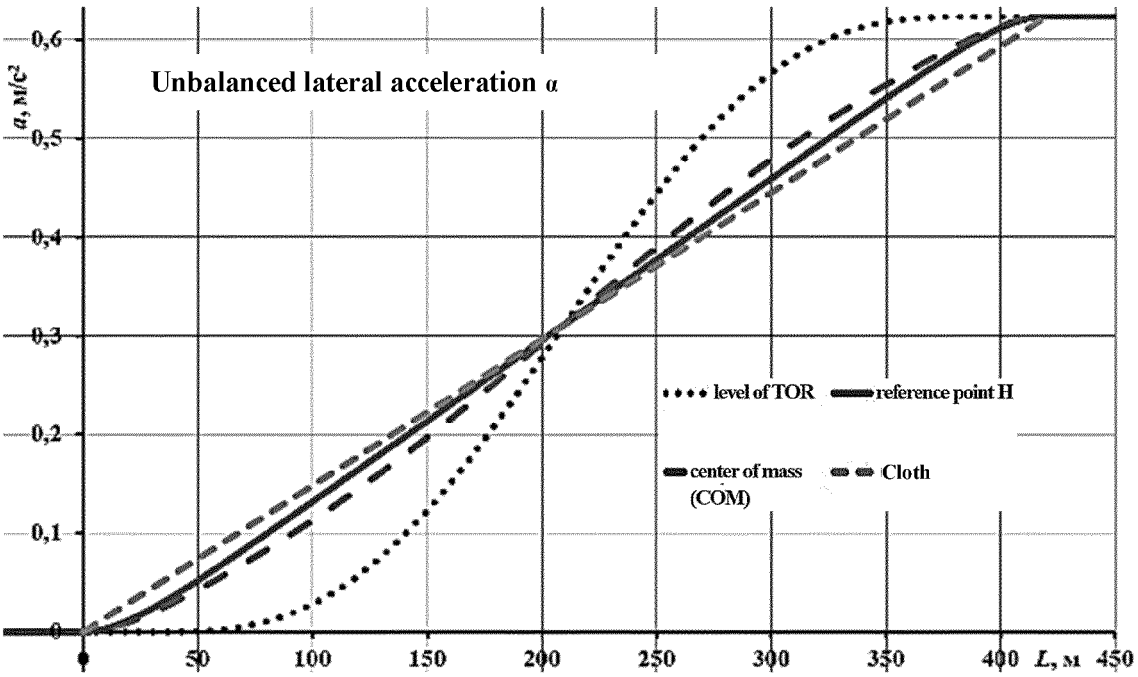
Unbalanced lateral acceleration α
a, м/с²
0,6
0,5
0,4
0,3
0,2
0,1
0
50
100
150
200
250
300
350
400
L, м
450
level of TOR
reference point H
center of mass (COM)
Cloth

FIG. 22

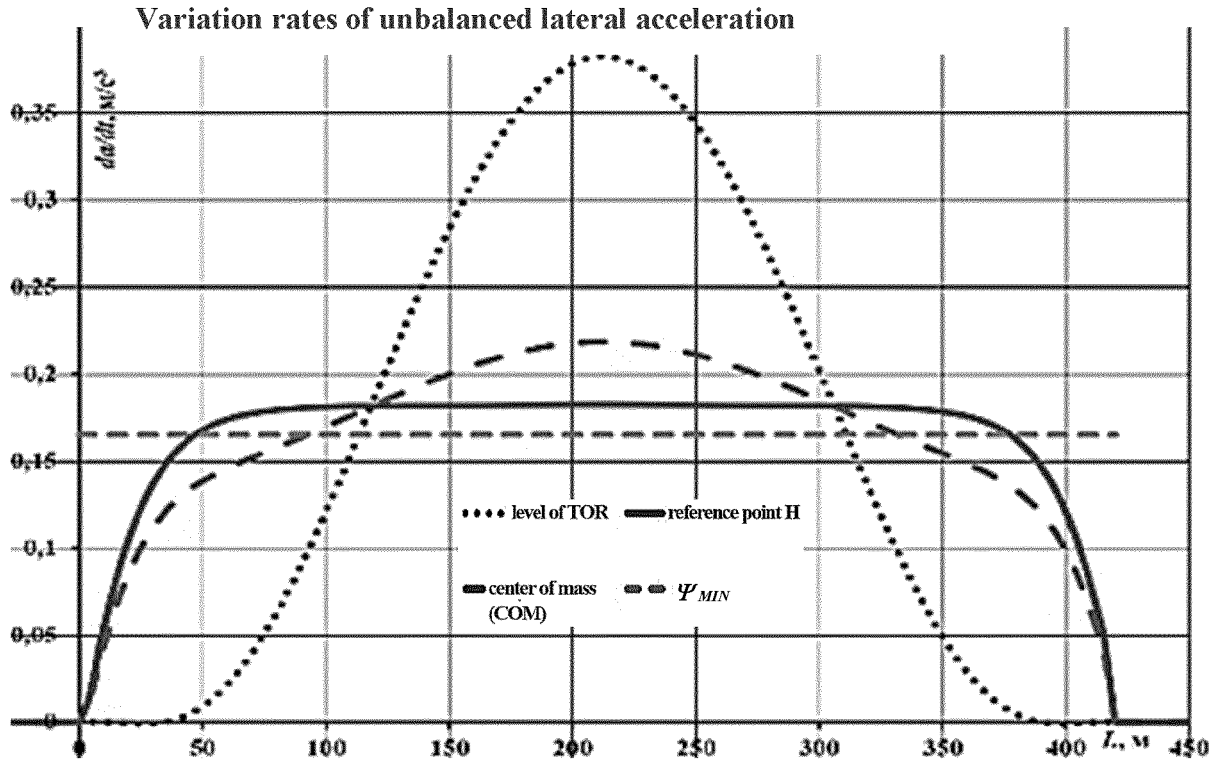
Variation rates of unbalanced lateral acceleration
da/dt, м/с³
0,35
0,3
0,25
0,2
0,15
0,1
0,05
0
50
100
150
200
250
300
350
400
L, м
450
level of TOR
reference point H
center of mass (COM)
Ψ MIN

FIG. 23

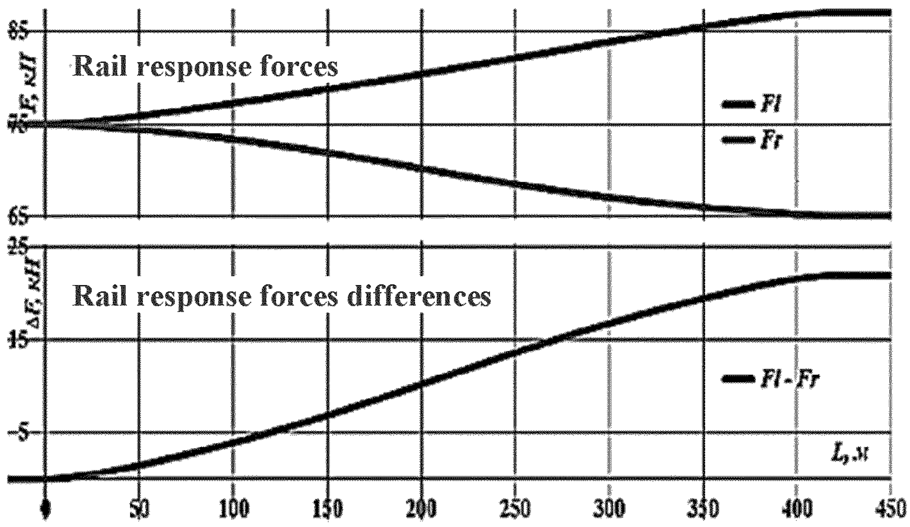
Rail response forces
F, кН
85
75
65
Fl
Fr
25
ΔF, кН
Rail response forces differences
15
5
Fl - Fr
L, м
0
50
100
150
200
250
300
350
400
450

FIG. 24

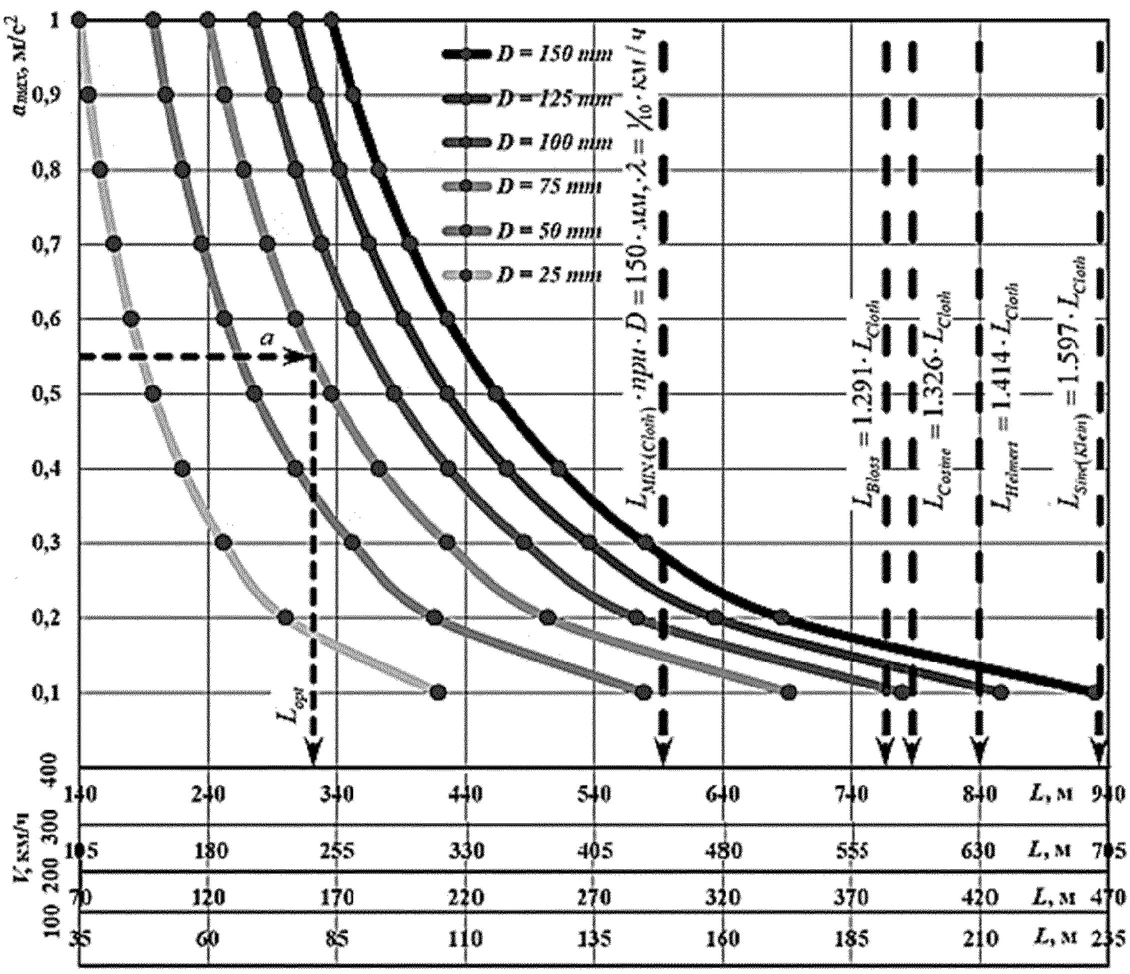
a_{max}, м/с²
1
0,9
0,8
0,7
0,6
0,5
0,4
0,3
0,2
0,1
D = 150 mm
D = 125 mm
D = 100 mm
D = 75 mm
D = 50 mm
D = 25 mm
a
L_{opt}
$L_{MIN(Cloth)} \cdot при \cdot D = 150 \cdot мм, \lambda = 1/10 \cdot км/ч$
$L_{Bloss} = 1.291 \cdot L_{Cloth}$
$L_{Cosine} = 1.326 \cdot L_{Cloth}$
$L_{Helmert} = 1.414 \cdot L_{Cloth}$
$L_{Sine(Klein)} = 1.597 \cdot L_{Cloth}$
V, км/ч
400
300
200
100
140 240 340 440 540 640 740 840 L, м 940
105 180 255 330 405 480 555 630 L, м 705
70 120 170 220 270 320 370 420 L, м 470
35 60 85 110 135 160 185 210 L, м 235

FIG. 25

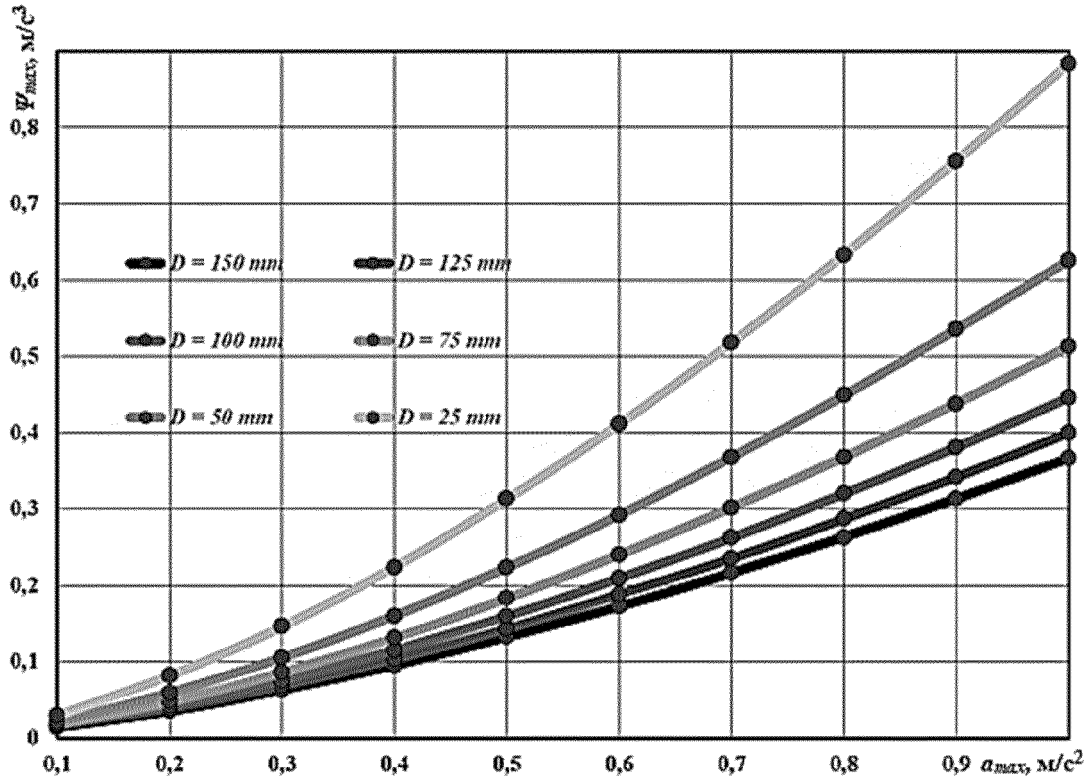
Ψ_{max}, м/с^3
0,8
0,7
0,6
0,5
0,4
0,3
0,2
0,1
0
D = 150 mm
D = 125 mm
D = 100 mm
D = 75 mm
D = 50 mm
D = 25 mm
0,1
0,2
0,3
0,4
0,5
0,6
0,7
0,8
0,9
a_{max}, м/с^2

FIG. 26

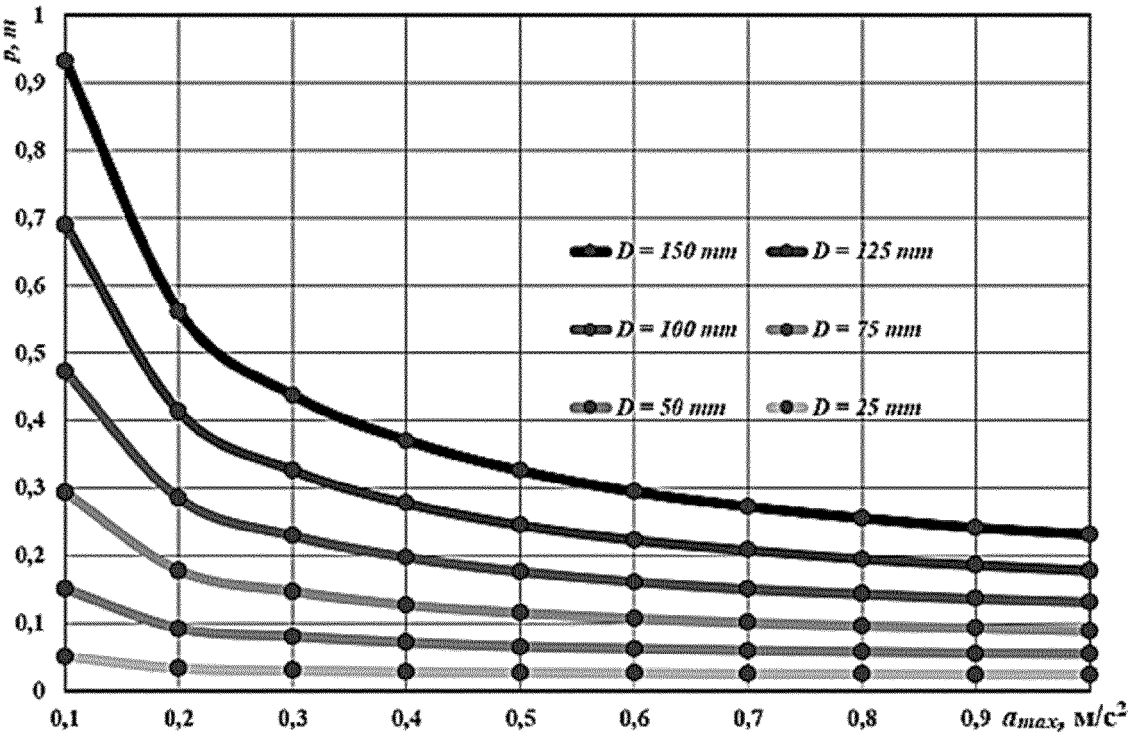
p, m
1
0,9
0,8
0,7
0,6
0,5
0,4
0,3
0,2
0,1
0
D = 150 mm
D = 125 mm
D = 100 mm
D = 75 mm
D = 50 mm
D = 25 mm
0,1
0,2
0,3
0,4
0,5
0,6
0,7
0,8
0,9
a_{max}, м/с^2

FIG . 27

INTERNATIONAL SEARCH REPORT

International application No.
PCT/BY 2022/000003

A. CLASSIFICATION OF SUBJECT MATTER
E01B 2/00 (2006.01) E01B 5/14 (2006.01)

According to International Patent Classification (IPC) or to both national classification and IPC

B. FIELDS SEARCHED

Minimum documentation searched (classification system followed by classification symbols)
E01B 2/00, 5/00, 5/02, 5/14

Documentation searched other than minimum documentation to the extent that such documents are included in the fields searched

Electronic data base consulted during the international search (name of data base and, where practicable, search terms used)
PatSearch (RUPTO internal), USPTO, PAJ, K-PION, Esp@cenet, Information Retrieval System of FIPS

C. DOCUMENTS CONSIDERED TO BE RELEVANT

Category*	Citation of document, with indication, where appropriate, of the relevant passages	Relevant to claim No.
A	WO 2001/098938 A1 (KLAUDER LOUIS T JR) 27.12.2001	1-3
A	VELICHKO G. Shape Harmonization of the Railway Track Transition Section & the Kinematics of Vehicle Body Design Point, In Transport Means 2020: Proceedings of the 24th International Scientific Conference, Part II, ISSN 2351-7034, p. 910-915	1-3
A	VELICHKO G. Quality analysis and evaluation technique of railway track + vehicle system performance at railway transition sections with various shape curves, In Transport Means 2020: Proceedings of the 24th International Scientific Conference, Part II, ISSN 2351-7034, p. 573-578	1-3
A	WO 2004/009906 A1 (WIENER LINIEN GMBH & CO KG et al.) 29.01.2004	1-3
A	AT 402211 B (OESTERREICHISCHE BUNDESBAHNEN) 25.03.1997	1-3

☒ Further documents are listed in the continuation of Box C. ☐ See patent family annex.

* Special categories of cited documents:
"A" document defining the general state of the art which is not considered to be of particular relevance
"E" earlier application or patent but published on or after the international filing date
"L" document which may throw doubts on priority claim(s) or which is cited to establish the publication date of another citation or other special reason (as specified)
"O" document referring to an oral disclosure, use, exhibition or other means
"P" document published prior to the international filing date but later than the priority date claimed
"T" later document published after the international filing date or priority date and not in conflict with the application but cited to understand the principle or theory underlying the invention
"X" document of particular relevance; the claimed invention cannot be considered novel or cannot be considered to involve an inventive step when the document is taken alone
"Y" document of particular relevance; the claimed invention cannot be considered to involve an inventive step when the document is combined with one or more other such documents, such combination being obvious to a person skilled in the art
"&" document member of the same patent family

Date of the actual completion of the international search	Date of mailing of the international search report
17 February 2022 (17.02.2022)	16 June 2022 (16.06.2022)
Name and mailing address of the ISA/ RU Facsimile No.	Authorized officer Telephone No.

Form PCT/ISA/210 (second sheet) (April 2005)

INTERNATIONAL SEARCH REPORT

International application No.
PCT/BY 2022/000003

C (Continuation). DOCUMENTS CONSIDERED TO BE RELEVANT

Category*	Citation of document, with indication, where appropriate, of the relevant passages	Relevant to claim No.
A	RU 2373318 C2 (KRAVCHENKO NIKOLAY DMITRIEVICH et al.) 20.11.2009	1-3

Form PCT/ISA/210 (continuation of second sheet) (April 2005)

REFERENCES CITED IN THE DESCRIPTION

This list of references cited by the applicant is for the reader's convenience only. It does not form part of the European patent document. Even though great care has been taken in compiling the references, errors or omissions cannot be excluded and the EPO disclaims all liability in this regard.

Patent documents cited in the description

- EP 1523597 B1 **[0066]**

Non-patent literature cited in the description

- Mathematical description of railway alignments and some preliminary comparative studies. **BJORN KUFVER.** VTI rapport 420A. Swedish National Road and Transport Research Institute, 1997 **[0066]**
- **KLAUDER, LOUIS, T., JR.** *Railroad curve transition spiral design method based on control of vehicle banking motion, https://patentscope.wipo.int/search/ru/detail.jsf?docId=WO2001098938&recNum=1&maxRec= &office=&prev Filter=&sortOption=&queryString=&tab= PC TDescription* **[0066]**
- **M. UENO et al.** Motion Sickness Caused by High Curve Speed Railway Vehicles. *Jpn J Ind Health,* 1986, vol. 28, 266-274 **[0066]**
- **VELICHKO, G.** Quality analysis and evaluation technique of railway track + vehicle system performance at railway transition sections with various shape curves. *Transport Means 2020: Proceedings of the 24th International Scientific Conference,* 2020, vol. 11, 573-578, https://transport-means.ktu.edu/wp-content/uploads/sites/307/2018/02/Transport-means-A4-II-dalis.pdf **[0066]**
- **VELICHKO, G.** Shape Harmonization of the Railway Track Transition Section & the Kinematics of Vehicle Body Design Point. *Transport Means 2020: Proceedings of the 24th International Scientific Conference,* 2020, vol. 11, 910-915, https://transport-means.ktu.edu/wp-content/aploads/sites/307/2018/02/Transport-means-A4-II-dalis.pdf **[0066]**
- *G.M. Shakhunyants Railway Track / G.M. Shakhunyants. - Moscow: Transport,* 1997, 479 **[0066]**
- **M.B. KURGAN ; D.M. KURGAN ; V. LAZARYAN.** Theoretical basis for the introduction of high-speed trains in Ukraine: monograph. Dnipro National University of Railway Transport - Dnipro, 2016, 283 **[0066]**
- **S.V. SHKURNIKOV et al.** Transport of the Russian Federation. *General Requirements to the Design of the Moscow-Kazan HSRL,* 2015, vol. 2 (57), 26-29 **[0066]**